1-1-2011

Investigating the structure and composition of anode-associated biofilms in electrochemical systems

Laura Berthiaume
Ryerson University

INVESTIGATING THE STRUCTURE AND COMPOSITION OF ANODE-ASSOCIATED BIOFILMS IN ELECTROCHEMICAL SYSTEMS

by

Laura Berthiaume
Bachelor of Science
Honours Biology
University of Windsor
2008

A thesis

presented to Ryerson University

in partial fulfillment of the

requirements for the degree of

Master of Science

in the Program of

Molecular Science

Toronto, Ontario, Canada, 2011

AUTHOR'S DECLARATION

I hereby declare that I am the sole author of this thesis. I authorize Ryerson University to lend this thesis to other institutions or individuals for the purpose of scholarly research.

_____

I further authorize Ryerson University to reproduce this thesis by photocopying or by other means, in total or in part, at the request of other institutions or individuals for the purpose of scholarly research.

_____

INVESTIGATING THE STRUCTURE AND COMPOSITION OF ANODE-ASSOCIATED BIOFILMS IN ELECTROCHEMICAL SYSTEMS

Laura Berthiaume
Master of Science, Molecular Science, Ryerson University, 2011

ABSTRACT

Microbial electrolysis cells (MECs) utilize microorganisms to catabolize organic substrates into biohydrogen and are being investigated as a potential solution to meet future energy needs. The focus of this project was to characterize the changes in microbial community composition of an anode-associated biofilm and to develop a method to monitor the biofilm *in situ* from an H-type, ethanol-fed MEC over the lifespan of the reactor. FISH and DGGE results revealed a shift in the biofilm microbial structure and composition from higher microbial diversity in the anaerobic digested sludge inoculum to a more uniform, lower diversity community towards the end of sampling. There was also an overall decrease in methanogenic community members and increase in both anode-respiring bacteria community, specifically *Geobacter* species, and current density over the time course, implying that a more stable community of anode-respiring bacteria, with minimal methanogens, results in higher current density and a more efficient MEC.

ACKNOWLEDGEMENTS

…..

I would like to thank my supervisor, Dr. Martina Hausner, for her support and guidance throughout this project. As well, Dr. William Yeung has been essential in helping me to develop my technical writing and laboratory skills throughout the last year. I would also like to thank Dr. Gideon Wolfaardt and Dr. Kim Gilbride for their input in developing and finalizing this project in my committee meetings. In addition, my collaborators from Arizona State University, Dr. Bruce Rittman, Dr. Prathap Parameswaran, and Dr. Cesar Torres, have all been important to this project by running the fuel cells and providing supporting data. Dr. Jesse Greener has been helpful in providing input in the embedding portion of the project. Lastly, I would like to acknowledge all the members of the Hausner and Wolfaardt lab for their knowledgeable suggestions in the last two years.

This research was supported by contributions from the Ryerson International Initiative Fund and NSERC.

TABLE OF CONTENTS

LIST OF TABLES

LIST OF FIGURES

LIST OF APPENDICES

LIST OF ABBREVIATIONS

APS	Ammonium persulfate
AEM	Anion exchange membrane
AFM	Atomic force microscopy
$BioH_2$	Biohydrogen
CEM	Cation exchange membrane
CLSM	Confocal laser scanning microscopy
DGGE	Denaturing gradient gel electrophoresis
FISH	Fluorescent *in situ* hybridization
FA	Formamide
HER	Hydrogen evolution reaction
HRT	Hydraulic retention time
LR White	London Resin White
MXC	Microbial electrochemical cell
MEC	Microbial electrolysis cell
MFC	Microbial fuel cell
MEGA	Molecular evolutionary genetics analysis
PBS	Phosphate buffered saline
PFA	Paraformaldehyde
PPMV	Parts per million by volume
PCR	Polymerase chain reaction
STM	Scanning tunnel microscopy

CHAPTER 1: INTRODUCTION

1.1. PROJECT SIGNIFICANCE AND MOTIVATION

The world has been focused mainly on fossil fuels as the major source of energy in the past century. As a result, the atmospheric carbon dioxide from burning fossil fuels has increased drastically. In 1959 when the atmospheric carbon dioxide was first measured at the Mauna Loa Observatory in Hawaii, atmospheric CO_2 was 316 ppmv. This has rapidly increased to 390 ppmv in 2010 (http://www.esrl.noaa.gov/gmd/ccgg/trends/). Continuing on this trend, the level of CO_2 is predicted to be 500 ppmv by 2100, raising global temperatures and exacerbating environmental damage (Logan, 2008). If this problem is going to be solved, society as a whole needs to search for more environmentally friendly alternative energies.

A variety of sources are already being investigated to replace traditional fossil fuel energy sources, including solar, wind and biomass. One of the potential new technologies used to harvest the energy stored in biomass utilizes microbial electrochemical cells (MXCs), specifically microbial fuel cells (MFCs) and microbial electrolysis cells (MECs). MFCs and MECs have become a well-studied alternative energy source in the last decade and are capable of utilizing microorganisms to oxidize an organic substrate to produce electricity or hydrogen, respectively (Holladay *et al.*, 2009).

More specifically, microbial fuel cells are units which utilize bacteria to catabolize organic material and generate an electrical current (Logan *et al.* 2006). There are several different MFC setups, but in general MFCs facilitate electron liberation from organic matter by microorganisms. The electrons travel through a series of respiratory enzymes and are eventually passed to the anode (negative terminal), where they become reduced. The electrons then travel through an external circuit, a conductive resistor, and finally to the cathode (positive terminal). In the

cathode chamber, electrons can then react with oxygen to form water (Du *et al.* 2007). In MECs, a modified microbial fuel cell, both the anode and cathode chambers are anaerobic and a small amount of external voltage is added in order to produce hydrogen gas. MECs facilitate an important form of bioenergy because they are carbon neutral, releasing only recently fixed carbon back into the atmosphere (Lovley, 2006) and hydrogen gas already has many applications where it can be used in place of fossil fuels (Lee *et al.*, 2010).

Currently one of the major hurdles in practically implementing MECs is that the power densities produced are still too low for most applications (Debabov, 2008). Research to improve these systems has focused mainly on the engineering aspect of the setups, with much less emphasis on the microbial communities that produce the current (Gupta *et al.*, 2011; Logan, 2009; Du *et al.*, 2007; Logan *et al.*, 2006). Much more research is still needed to better understand the electricity-producing microorganisms that power MECs in order to employ large-scale versions. Specifically, how anode-associated microorganisms transfer electrons from a substrate to the electrode and what microbial community members do this most efficiently. The work in this investigation examines how a mixed community, developed from anaerobic digested sludge, changes over time and how this correlates to current density. It is part of a collaborative effort with Arizona State University's Center for Biotechnology and compliments work done previously to investigate syntrophic relationships between organisms at the anode (Parameswaran *et al.*, 2010).

1.2. OBJECTIVES AND THESIS OUTLINE

Microbial electrolysis cells (MECs) are a promising source of biohydrogen for the future. However at present, H_2 production within these units is too low to meet the world's increasing energy demands. In order to improve MEC function and allow for practical implementation, there needs to be a clearer understanding of the roles microorganisms play in current production. This will allow for the capability to engineer an optimal current producing microbial community and maximize biohydrogen production.

The scope of this work was designed to address the overall goal of this study, namely to describe the microbial community composition in an anode-associated biofilm within an H-type microbial electrolysis cell (Chapter 2) and develop a method to observe the biofilm *in situ*, on the electrode (Chapter 3). It was also critical to establish any time-resolved changes in the biofilm over the lifetime of the MEC reactor to better understand temporal MEC community dynamics. This was accomplished by completing two overall goals; (i) using 16S rRNA PCR-denaturing gradient gel electrophoresis (DGGE) and fluorescent *in situ* hybridization to characterize and quantify the anodal biofilm communities at different temporal stages of the MEC reactor, and (ii) developing an embedding protocol to characterize the MEC biofilm using fluorescent probes *in situ* on the electrode.

1.3. EXPECTATIONS

As mentioned previously, the main hurdle in practically implementing MECs is that the cost of system set up and operation is still high compared to the amount of biohydrogen produced. It is expected that the results of this investigation will increase knowledge of the anode-associated microbial communities within MECs, specifically regarding how the composition and structure affects current density in an H-type MEC inoculated with anaerobic digested sludge. This is in attempt to eventually improve overall MEC functioning and increase BioH_2 production so that this environmentally friendly setup can be utilized to its full potential and the replace a portion of more traditional fuel sources.

The expectations of the composition of the microbial community are based on prior research of the final anodal community by our collaborators (specifically, Parameswaran *et al.*, 2009, 2010), indicating there will most likely be *Bacteria* and *Archaea,* from a few specific taxa present in the MEC. It is also likely that the current density will increase when more anode respiring bacteria (ARBs), microorganisms able to transfer electrons contained in organic substrates to a solid electrode, are present in the community, since ARBs are responsible for transferring electrons directly from a substrate to current. As well, it is expected that there will be a decrease in current density when there are more methanogens present because these microorganisms divert electrons to methane production rather than current. It is also probable that there will be an overall shift towards more ARB as the reactor runs longer, since current density usually increases over time in MECs. Lastly, it is anticipated that there be different *Proteobacteria* present in the anode-associated community based on previous studies which have indicated their prevalence in MEC communities (Aelterman *et al.*, 2006; Logan, 2008; Chae *et al.*, 2010).

1.4. LITERATURE REVIEW

1.4.1. Microbial Electrolysis Cell Principles

Microbial electrochemical cells (MXCs) have become an intensely discussed area within the last decade as an environmentally friendly alternative fuel source (Gupta *et al.*, 2011; Logan, 2009; Du *et al.*, 2007; Logan *et al.*, 2006). The term MXC describes a category of reactors that exploit the capability of certain anaerobically grown microorganisms to catabolize organic material, liberate electrons and directly transfer electrons to an electrode within a battery-type system. (Logan *et al.* 2006). The electrons travel through a series of respiratory enzymes and are eventually passed to the anode (negative terminal), the electrons then travel through an external circuit, a conductive resistor, and finally to the cathode (positive terminal). In the cathode chamber, electrons can react with oxygen to form water. In microbial electrolysis cells, a specific type of electrochemical system, oxygen is removed from the cathode chamber and a small amount of external voltage, theoretically 0.14 V but practically approximately 0.3 V, is added in order to enable the reduction of protons (H^+) to H_2 gas, allowing the process of electrolysis to occur. This is when electricity is used to drive a non-spontaneous reaction (Borole and Mielenez, 2011). Anode, cathode, and overall reactions for an MEC are shown below, with acetate as the model electron donor:

e^- donor half reaction: $CH_3COO^- + 3\ H_2O \leftrightarrow CO_2 + HCO_3^- + 8\ H^+ + 8e^-$ -0.29 V
(at the anode)
e^- acceptor half reaction: : $8\ H^+ + 8\ e^- \leftrightarrow 4\ H_2$ -0.41 V
(at the cathode)

Net reaction: $CH_3COO^- + 2\ O_2 = CO_2 + HCO_3^- + H_2O$ -0.12 V

The relationship $\Delta G = -nF\Delta E$ converts the net potential difference (ΔE) into a net Gibbs free energy change (ΔG). Reactions are only feasible when ΔG is negative, and hence the converse is true for ΔE. In the case of an MEC, the overall ΔE is -0.12V, which means that energy has to be applied to the system, theoretically slightly more, to favour hydrogen production. Fig. 1.1 shows the full process of biomass conversion to biohydrogen, using plant waste as an example substrate.

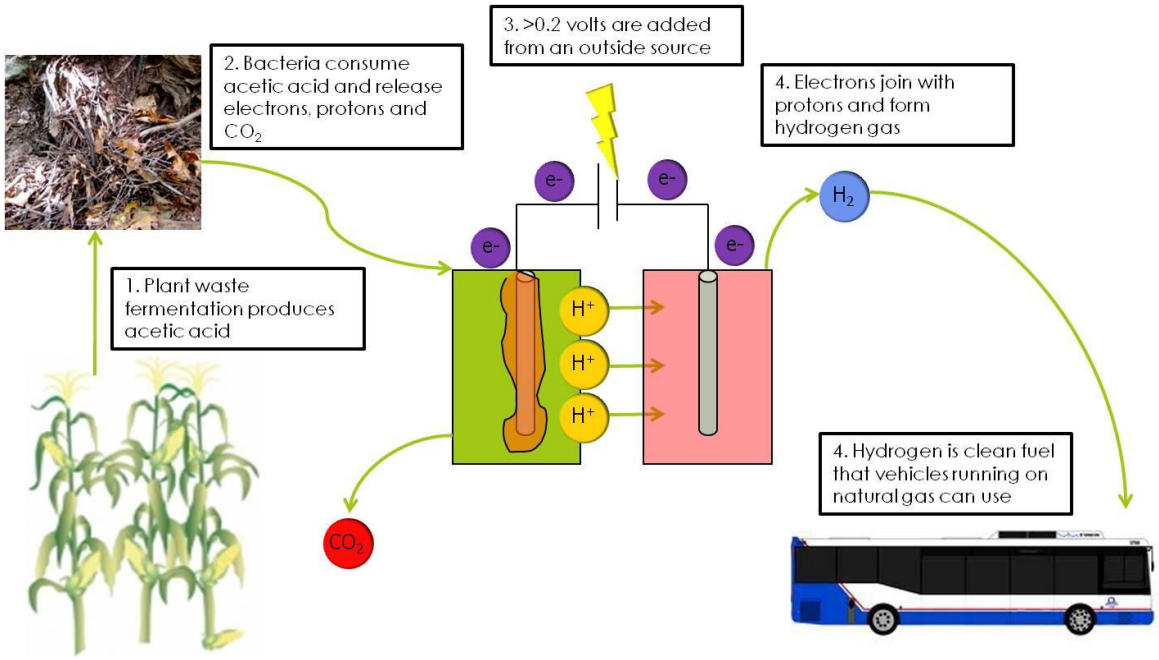

Fig. 1.1. The process of producing biohydrogen in a two-chamber microbial electrolysis cell using plant waste as a substrate.

There are several advantages to employing MECs as a bioenergy source. Firstly, the MEC is carbon neutral process, since is releases only recently fixed CO_2 (Du *et al.*, 2007). Also, MECs generate hydrogen from biodegradable materials, ranging from pure compounds such as acetate and glucose to complex mixtures of organic matter including municipal, agricultural, and food-related wastewaters that would otherwise not serve a purpose. Another factor that makes MECs attractive is the wide variety of uses for biohydrogen ($BioH_2$), specifically the potential for its

use in vehicles (Cheng and Logan, 2011). BioH_2 can also be used in bioremediation by acting as an electron donor to reduce water pollutants including nitrates and can be used for the hydrogenation many products, including gasoline and fertilizer (Lee *et al.*, 2010).

Current production in MECs is dependent on four factors: (i) efficiency of microbial catabolism, (ii) anode performance, (iii) cathode performance and (iv) proton transfer from the anode to the cathode. Each of these aspects and their role in power generation will be discussed in the following sections.

1.4.2. Microbial Electrolysis Cell Materials

There are a wide variety of materials currently being investigated for their use in MECs. This section will review the three most important parts of an MEC where material research is being investigated: the anode, cathode and proton exchange membrane. The main research focus with all three is low-cost and high-efficiency.

1.4.2.1. Anode

The material used for the anode must fit a number of highly specific criteria: conductive, large surface area, inexpensive, chemically stable in buffer solutions, non-corrosive and has the potential to be scaled up. They most commonly consist of carbon-based materials, found in many forms, because they are highly conductive and porous. They can also be sanded to increase the surface area for colonization. Different varieties include carbon cloth, carbon paper, carbon foam, graphite felt, graphite granules, and graphite brushes (Logan *et al.*, 2008). Also, shown to increase anode performance is the treatment of carbon-based electrodes with high temperature ammonia gas resulting in a faster reactor start-up, thought to be caused by microorganisms adhering quicker to the anode and improved electron transfer (Logan *et al.*, 2008). The most efficient MEC design utilizes a graphite brush for the anode and no membrane separator (Show

et al., 2011). This membraneless design decreased the necessary voltage from 0.5 V with a Nafion membrane to 0.4 V, resulting in increased efficiency from 53% to 76%. The hydrogen production rate in this unit was found to be 3.12 m^3/m^3reactor/day (Call and Logan, 2008).

Other materials have also been investigated for use as the anode but with less success than carbon-based electrodes. Conductive polymers have not been used extensively but research has shown that polymers are not as effective as carbon paper or cloth. Metal and metals coatings have also been investigated but with disappointing results (Logan, 2006). So far aluminium oxide, iron oxide, stainless steel, titanium and tungsten have been tested, with studies concluding that they can only generate a fraction of the current that MECs with either carbon-based or graphite electrodes have been shown to produce (Logan, 2006).

1.4.2.2. Cathode

The reaction within the cathode chamber has been a challenging area of microbial electrolysis cells to work on. This is where hydrogen production occurs, also known as the hydrogen evolution reaction (HER) (Cheng *et al.*, 2006). When the HER takes place using carbon electrodes, it is slow and requires a high overpotential, which is the potential difference between a half-reaction's theoretically determined reduction potential and the potential at which the redox event is experimentally observed (Bard and Faulkner, 2000). Researchers have seen a reduction in overpotential by using a platinum catalyzed electrode, which can be bought or made in the lab by binding commercial platinum to a carbon electrode. The main disadvantage to this approach is the high cost of platinum and the negative environmental impacts of mining it (Freguia *et al.*, 2007). Platinum's efficiency also has been negatively impacted by certain compounds found in waste products, such as sulphide (Selembo *et al.*, 2009).

More recently, researchers have been using biocathodes to catalyze the HER, where the reaction is catalyzed by bacteria. This method was originally developed by the Rozendal group in 2008 and has yet to be fully optimized. Currently biocathodes are created by enriching electrochemically active, hydrogen-oxidizing bacteria on the anode, followed by reversing the polarity of the electrode (Rozendal *et al.*, 2008). The original test biocathodes had a current density of 1.1 A/m^2, compared to a regular graphite cathode, which only had a current density (the amount of current produced per unit area) of only 0.3 A/m^2. What is also interesting is that the same group was able to develop additional biocathodes by inoculating them with the effluent of an already active biocathode, demonstrating that subsequent generations of biocathodes produced this way can produce a similar current density (Rozendal *et al.*, 2008). Biocathodes are becoming a promising alternative due to their low cost and high performance.

1.4.2.3. Membranes

Currently most MECs contain a membrane separating the anode and cathode chamber, although various research groups do use single-chamber MECs (Call and Logan, 2008; Hu *et al.*, 2008; Lee *et al.*, 2009). The purpose of a membrane is to separate the microorganisms being used in the cathode chamber from those in the anode chamber. This reduces the crossover of fuels and bacteria between the two chambers and helps maintain the purity of the hydrogen gas evolved at the cathode (Liu *et al.*, 2010). Generally the membrane minimizes hydrogen losses to hydrogen scavengers found in the anode-associated community and prevents mixing of hydrogen gas with carbon dioxide produced at the anode, while selectively allowing proton to move from the anode chamber to the cathode (Rozendal *et al.*, 2006).

Many of the first MECs used a cation exchange membrane (CEM) such as Nafion 117 (Logan *et al.*, 2008). The main problem with these CEMs is that they allow cation species besides protons

through the membrane. These include Na^+, K^+, NH_4^+, and Ca^{2+}, all of which are found in wastewater at pH 7 and present in 10 times higher concentrations than protons (Liu *et al.*, 2005). This results in a pH increase at the cathode and decrease at the anode because the protons consumed at the cathode are not replaced.

Other types of membranes that have been tested include anion exchange membranes (AEMs) bipolar membranes (BPMs) and charge mosaic membranes (CMMs). Of note in MEC research recently are AEMs due to their ability to transport negatively charged chemical buffers (phosphate or bicarbonate) across the membrane (Cheng and Logan , 2007). This helps to buffer pH changes in the two chambers, resulting in hydrogen production at a rate of 1.1 m^3H_2/m^3day with a graphite granule anode.

The disadvantages of most membranes are their high cost, some as high as \$1400/m^2. They also may increase the internal resistance of MEC systems. This is due to decreased proton diffusion to the cathode compared to a system with no PEM. In systems where the electrodes are spaced closely together there is a more pronounced increase in internal resistance, compared to those where the electrodes are farther apart (Kim *et al.*, 2007).

The different materials described in the section above can be arranged in a number of ways. This is referred to as the architecture of the system, described in the following section.

1.4.3. Microbial Electrolysis Cell Architecture

The current research focus of system architecture is scaling up MECs for a variety of practical applications. Currently there are no models that are economical enough to implement into industrial applications with the exception of small-scale sediment microbial fuel cells, which power small monitoring devices in remote locations (Lovley, 2006). Industrial implementation of MECs requires the system architecture to be cost effective to mass produce, efficient, and stable.

This section will review the two general system setups, one-chamber and two-chamber systems, and factors that affect their scalability.

1.4.3.1. Two-chamber Microbial Electrolysis Cells

Two-chamber aqueous cathode MECs are the most common setups for these reactors because they are relatively simple in design and permit for a variety of factors to be tested for their affect on power production. This system has two chambers separated by a membrane to create a potential difference. The chambers can be either bottle-type, cube-type, disc-type, or rectangular and are maintained under anaerobic conditions, shown in Fig. 1.2 (Liu *et al.*, 2010). Organics are injected into the anode chamber under anaerobic conditions, where the ARBs exist. The hydrogen is produced at the cathode and is collected at the headspace (Rozendal *et al.*, 2008). The main hurdle with this system is in having to use a membrane, resulting in high internal resistance. This is thought to be the reason for low current densities (0.2–3.3 A/m^2) and hydrogen-production rates (0.015 –1.1 $m^3/day/m^3$) in this setup (Liu *et al.*, 2010).

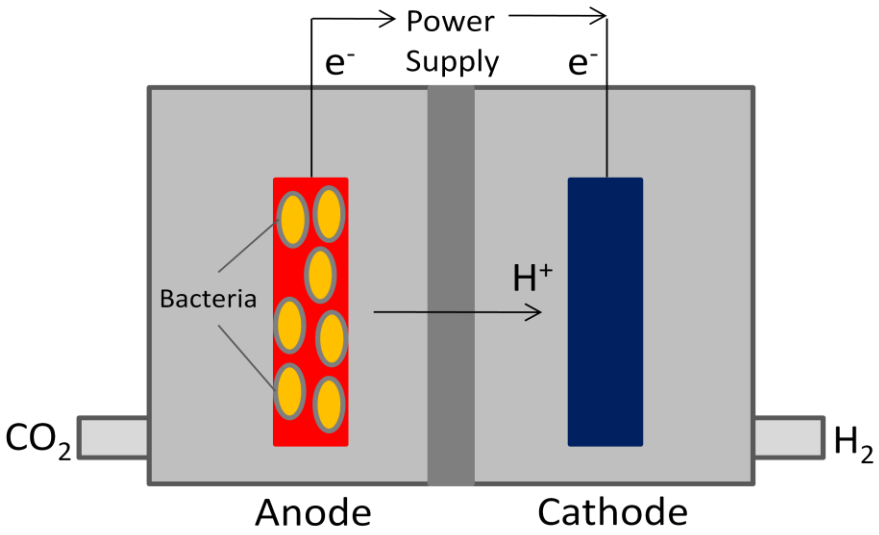

Fig. 1.2. A standard membrane separated two-chamber microbial electrolysis cell.

1.4.3.2. One-chamber Microbial Electrolysis Cells

Single-chamber MECs are a more recent development, where both the anode and cathode are submerged in solution within one compartment, typically made of glass or plastic, shown in Fig. 1.3 (Call and Logan, 2008). This an easy and less expensive setup to alternatives where membranes are used and allows for easy manipulation of various power generation factors (Du *et al.*, 2007). Another advantage of using single-chamber MECs is that the removal of membrane can reduce the potential loss caused by the membrane resistance, resulting in increased current density (4.2–12 A/m^2) and a faster HER (0.5–3.1 $m^3/day/m^3$) (Liu *et al.*, 2010).

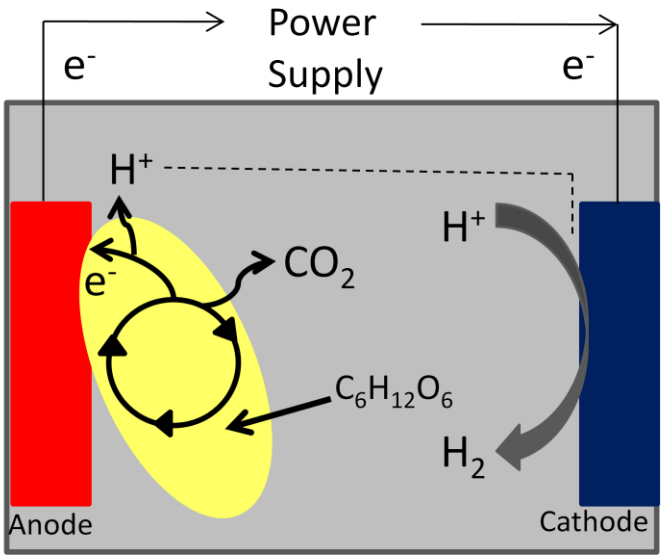

Fig. 1.3. A single-chamber membraneless microbial fuel cell schematic.

The major hurdle with these single-chamber systems is that often hydrogen scavengers in the anode community consume the hydrogen produced at the cathode since the gases are not separated as in a two-chamber MEC. Although the HER may occur more quickly at the beginning of the setup, research has shown that within weeks of startup, there is an eventual increase in methane production and decrease in hydrogen production. This is mainly due to the catalytic activities of hydrogenotrophic methanogens (Hu *et al.*, 2008). Various methods have

been investigated to prevent methanogensis including exposing cathodes to air periodically, employing only pure cultures at the anode, and lowering the MEC solutions pH, all with limited success (Liu *et al.*, 2010). Future single-chamber MEC research efforts should be focused on utilizing highly efficient or genetically modified ARBs, as well as mixed bacterial cultures with reduced hydrogen scavengers. The research of MEC microbial communities will be discussed in more detail within the next section.

1.4.4. Microbial Electrolysis Cell Microbial Communities

Electricity production by microbial communities was originally discovered by Potter (1912), who was the first person to investigate the principles of modern day electrochemical cells. A small amount of electrical energy was produced by employing *Escherichia coli* and *Saccharomyces cerevisae* within an electrochemical system using platinum electrodes (Potter, 1912). These findings were not utilized for another 70 years, until the 1980s, when it was discovered that electricity generation could be greatly increased by adding artificial mediators (Du *et al.*, 2007). Due to the toxicity and high cost of these exogenous mediators, MXC research slowed again for another 10 years, until 1999, when it was discovered that certain microorganisms could efficiently transfer electrons in the absence of mediators (Kim *et al.*, 1999; Chaudhuri and Lovley, 2003). The first organisms found to do this were *Shewanella putrefaciens*, *Geobacteraceae sulferreducens*, *Geobacter metallireducens* and *Rhodoferax ferrireducens*. All were found to be bioelectrochemically active and able to form a biofilm on the anode surface, allowing for unmitigated electron transfer (Debabov, 2008).

Currently, most MEC research now focuses on mixed communities but some research groups still work with pure cultures because it is easier to see how changes to the setup affect power output, since changes in current density will most likely be the result of reactor component

changes and not community fluctuations. Pure cultures can also be used as model organisms to investigate complete oxidation of particular organic compounds and electron transfer mechanisms. The most common model organisms are species that were used in original MXC work, *Shewanella putrafaciens,* a few different *Geobacter* species, most commonly *Geobacter sulfurreducens,* and *Rhodoferax ferrireducens,* because *R. ferrireducens* has an over 80% electron recovery rate and has the ability for long-term survival under starvation (Lovley, 2006).

Although pure cultures are valuable in certain investigations, at present the highest current density has been seen in MECs with mixed microbial communities (Logan and Regan, 2006). This is most likely due to the fact that a greater diversity in organisms usually translates into a broader spectrum of substrates that can be utilized. These mixed anodal communities form a biofilm on the anode from a variety of sources including untreated wastewater (food-processing, meat processing, municipal), wastewater sludge, and river sediment, among others (Du *et al.*, 2007). In general, MEC biofilms are a thick, electrochemically active community located on the anode, consisting of a variety of microorganisms, namely ARBs and fermenters, which cooperate syntrophically to generate current (Parameswaran *et al.*, 2009).

The sections below will discuss current research on mixed MEC communities; more specifically the two most common types of bacteria that develop in mixed communities, as well as the more recent use of microorganisms at the cathode.

1.4.4.1. Energy Extraction from Biomass

Microorganisms are able to grow and gain energy by transferring electrons through a series of trans-membrane complexes during the process of respiration. In doing so, the electrons create a proton gradient across the cellular membrane. Although it is not know yet exactly what cellular proteins are involved in electron transportation from electron carriers to the anode, various

groups have proposed mechanisms for metal reducing microorganisms using intracellular membrane proteins (Du *et al.*, 2007). Once the electrons are passed to the anode, they move towards a final electron acceptor, which can range from oxygen, nitrate, iron, or sulphate, among others. Fundamentally, bacteria search for the acceptor with the highest redox potential to increase their energy for growth (Logan, 2006). This explains a microorganism's incentive to search for alternative electron acceptors and the basis for MECs. The organisms capable of performing energy extraction, specifically two of the main groups found in mixed communities within MECs, will be discussed in the next two sections.

1.4.4.2. Anode Respiring Bacteria

MXC research accelerated following a 2001 publication, revealing the successful use of an MFC to power small electronic equipment in hard to access areas for several years without problem (Du *et al.*, 2007). In this setup, the anode was submerged in anaerobic bottom sediment and a cathode in seawater containing dissolved oxygen, both graphite electrodes, reaching a power of $0.01 W/m^2$ (Reimer *et al.*, 2001). Following this discovery, the Lovley group replicated the setup in the lab to further investigate this community that could function with no external additives, including mediators or substrates. They noted the current production was due to a mixed community comprised mainly of *Proteobacteria*, specifically members within the family *Geobacteraceae,* and that these organisms were capable of direct electron transfer (Debabov, 2008). It is now known that there are several species which are able to transfer electrons directly to the anode in an MEC. They are collectively known as anode respiring bacteria (ARBs), exoelectrogens, or electricigens (Lovley, 2006). For the sake of consistency, they will be referred to as ARBs throughout this thesis.

In general, ARBs work at the anode, hydrolyzing complex organic substrates and transferring liberated electrons to the anode. The overall anodal reaction involves the combination of an organic substrate plus water giving carbon dioxide, protons and electrons (Logan, 2006). It has been shown that ARBs can be enriched from various environments, including sludge, sediment and wastewater and belong to diverse genetic groups, including the alpha, beta, delta and epsilon classes of the *Proteobacteria*, the phyla *Firmicutes*, *Acidobacteria* and *Actinobacteria* (Liu *et al.*, 2010). The liberated electrons can be transferred from ARBs to the anode by one of three known mechanisms, endogenous shuttles, direct anodal contact or nanowires (Logan, 2009), which are all discussed in more detail in section 1.4.5.

It is also interesting to note that so far, community analysis of MEC biofilms shows that there is no single ARB within a bacterial community that performs better than a mixed community (Lovley, 2008). This is due to the fact that several different bacteria are capable of electricity production and a wider array of microorganisms can utilize a greater diversity of complex substrates, such as those found in wastewater. Also, mixed communities can often adapt better to changing environments, including pH and temperature fluctuations (Angenent and Wrenn, 2008). Aside from ARB, fermenters have been shown to play an important role in current production within mixed MEC communities, which is discussed in the next section.

1.4.4.3. Fermentative organisms

Anaerobic metabolism is preferred within MECs in order to convert organic matter to BioH_2. One type of anaerobic metabolism performed in the anode chamber is fermentation. Fermentative organisms break down complex organic substrates, producing mostly smaller molecules such as acetate and other fermentation products. These compounds cannot react with the anode but contain the electrons necessary for power production, therefore requiring further

oxidation (Rabaey *et al.* 2006). However, despite the inability for direct electron transfer, fermentation appears to be an important process for the utilization of complex organic substrates, alcohols, and simple acids other than acetate (Kim *et al.*, 2007; Liu *et al.*, 2005; Ren *et al.*, 2007; Torres *et al.*, 2007).

The most effective anaerobic oxidation process requires the cooperation of fermenters, as well as other organisms which can utilize subsequent fermentation products including hydrogen, acetate, and other minor acids, further metabolizing the products to liberate the electrons contained within these compounds. Several studies have shown that most substrates are primarily fermented when complex organic wastes are used, since there are usually a percentage of fermenters within the anode chamber (Ren *et al.* 2007; Richter *et al.*, 2008). Acetate and other more minor fermentation acids are then completely oxidized to carbon dioxide by other non-fermenters, primarily ARBs (Lovley, 2006).

1.4.4.4. Cathode Associated Microorganisms

Certain microorganisms are capable of reducing protons at the cathode to facilitate the hydrogen evolution reaction (HER) (Jeremiasse *et al.*, 2010). Since these microbes are not necessary for MEC function, they have been investigated much less than those present at the anode. However, studies using bacteria as electron-oxidizers have become more popular since other means of HER catalysis, namely platinum electrodes, are so costly (Jeremiasse *et al.*, 2010). At present, limited community analyses have been performed on these communities, so far indicating only the presence of species within the genera *Pseudomonas* and *Novosphigobium* (Clauwaert *et al.*, 2007).

What has also interested MEC researchers is the possibility of bioremediation within the cathode chamber. Istok *et al.* (2010) discovered that certain bacterial strains could reduce harmful

compounds such as uranium (VI), nitrate, and chlorinated compounds, using electrodes as the sole electron donors. One strain, *Geobacter lovelyi,* can reduce chlorinated compounds with an electrode serving as the sole electron donor (Gregory *et al.*, 2004).

The microbiology of bioremediation within the cathode chamber has not yet been investigated in detail but it does offer potential advantages for bioremediation of certain contaminants over more traditional approaches. Another proposed idea is nitrate removal from wastewater via direct electron transfer from electrodes to denitrifying microorganisms. While this is an interesting concept, further research is still needed to determine if it is feasible (Lovley, 2008).

After discussing the various organisms present within MECs, the next section will outline the proposed methods that these MEC microorganisms use to transfer harvested electrons.

1.4.5. Electron Transfer

There are currently four speculated modes of electron transfer from bacteria to the anode. The first three all involve utilizing the cellular mechanisms, while the fourth requires the use of mediators, which can be either artificial or a product of the microorganisms. At this point, little is known about the mechanisms for electron transfer, especially because of the variety of species used in MECs, and further understanding of these mechanisms will help to improve MEC design and functioning.

1.4.5.1. Mediators

The outer layer of most cellular membranes are comprised of components which hinder direct electron transfer to the anode including a non-conductive lipid membrane, peptidoglycans and lipopolysaccharides. One possible pathway for the electrons to reach the anode is via electron mediators, exogenous low-molecular weight electron transporters which accept electrons within a cell or on the cell surface and releasing them at the electrode (Debabov, 2008). More

specifically, oxidized mediators are able to penetrate outer cell lipid membranes and the plasma wall and interact with reducing agents such as NADH, NADPH and reduced cytochromes, to become reduced. The mediators then carry the electrons from the electron transport chain that would normally be taken up by oxygen or other intermediates to the anode where they become oxidized again and are ready to repeat the process (Logan, 2006). There are five main requirements for the MEC mediators: 1. They can pass through or be absorbed by the microbial cytoplasmic membrane; and 2. They should be soluble in aqueous systems; 3. They are non-biodegradable or toxic to the organisms; 4. They are low cost; and 5. They react quickly at the anode (Du *et al.*, 2007). There are two categories of MEC mediators, artificial and endogenous. Below each will be described in more detail.

1.4.5.1.1. Artificial Mediators

Artificial mediators were more commonly used in earlier microbial fuel cell setups. Researchers would add a variety of different chemicals to the anode chamber in order to facilitate electron transfer. These included neutral red, anthraquinone-2,6-disulfonate, thionin, potassium ferricyanide, and methyl viologen (Logan, 2008). These compounds have been mostly phased out of MEC research because they are expensive and require replenishing; as well they are all toxic to work with. Most setups now utilize bacteria that are able to transfer electrons independently of artificial mediators, through either endogenous mediators, direct, or long-range electron transfer to the anode.

1.4.5.1.2. Endogenous Mediators

It was the Rabaey group who first demonstrated that expensive, toxic mediators were not necessary for electron transfer. They were able to show that certain organisms could self-produce redox mediators (Rabaey *et al.*, 2005, 2004). This pioneer work on endogenous mediators was

done using *Pseudomonas aeruginosa*, which produces pyocyanin, a small molecule that is capable of shuttling electrons to the electrode (Rabaey *et al.*, 2004). They were also able to demonstrate that pyocyanin produced by one organism can be used by other members in a community. This was shown by the addition of pyocyanin to two pure cultures, *Lactobacillus amylovorous* and *Enterococcus faecium*, resulting in an in power output using the exact same system architecture and components, except pyocyanin was removed (Rabaey *et al.*, 2004).

At present, it is not entirely evident why *P. aeruginosa* produces pyocyanin. While it does actually shuttle electrons, pyocyanin can also perform antibacterial activities and it may be secreted to kill competitors within a community. In one experiment performed by Rabaey *et al.* (2005), addition of pyocyanin to an anode chamber which contained a pure culture of *Escherichia coli* decreased power output by killing some of the viable cells.

At this point, there have been other organisms discovered that self-produce endogenous mediators including *Shewanella oneidensis*, which is known to synthesize a suite of potential endogenous redox mediators including menaquinones, flavins and ubiquinones (Lies *et al.*, 2005; Myers and Myers, 2004; vonCanstein *et al.*, 2008). Lastly, *Geothrix* (Nevin and Lovley, 2002), *Lactobacillus* and *Enterococcus* (Rabaey *et al.*, 2004) species have also been shown to secrete soluble electrochemically active molecules.

1.4.5.2. Direct Anodal Contact

Another proposed method of conductivity occurs when microbes are in direct contact with the anode. In this proposed mechanism, electrons reach the outer membrane of the cell and then are transferred to the electrode via outer-surface c-type chromosomes (Lovley, 2008). In the case of aerobically grown metal-reducing bacteria, the cytochrome content of the cytoplasmic membrane is usually 10–30 times higher than that of the outer membrane, supporting this theory. Although

this ratio decreases under anaerobic growth conditions, the cytochromes still remain localized predominantly in the cytoplasmic membrane (Logan, 2006). This was first shown using advanced spectroelectrochemical studies with *Geobacter sulfurreducens* (Logan, 2006). Although the exact proteins involved in this method have not been determined, researchers have found strong adherence to electrodes under anaerobic conditions two to five times stronger than in aerobic environments, as well as small molecules surrounding the bacteria present on electrons micrographs (Lower *et al.*, 2001).

1.4.5.3. Nanowires

Other research groups are more focused on investigating the mechanisms behind long range electron transfer, when biofilms formed on the anode become thicker than 50μm. This has been shown to occur using conductive appendages or pili, now referred to as nanowires (Lovely, 2008).

Gorby and Beverage were the first to coin the term nanowire when they noticed the presence of conductive appendages present on *Shewanella* species. They determined this using conductive scanning tunnel microscopy (STM), where a bacterial sample is loaded onto a flat, highly conductive surface. A conductive tip is then moved across the sample under constant-current imaging conditions. The current-voltage then changes according to how conductive that portion of the scan is relative to the surface. Gorby and Beverage noticed that the current increased as the tip passed over the appendages, indicating conductivity (Logan *et al.*, 2006). Gorby was also able to perform knockout studies to determine the genes responsible for electron transfer within these conductive appendages. He noted that mutants missing certain respiratory cytochromes, specifically those produced by the genes *mtr*C and *omc*A, produced appendages but they were

not conductive when STM scans were performed or able to produce electricity in MECs (Gorby *et al.,* 2006).

Further nanowire research has also been performed using species within the *Geobacter* genus. Reguera was also able to show conductivity with *Geobacter* appendages, but in this instance used conductive Atomic Force Microscopy (AFM). It was noted that there were also conductive appendages generated by *Geobacter*, however they are actually significantly different than those produced by *Shewanella*. *Geobacter* produce very thin, individual strands, while Shewanella species produce bundles of thick wires. (Reguera *et al.*, 2005)

1.6. Future research needs for the optimization of microbial electrolysis cell performance

While it is possible that MECs will eventually be used as a large-scale source of power, in the short term it is most likely that these reactors will be used to power small electronic devices and waste water treatment. Practical applications are still generally limited by the efficiency of biohydrogen production, the cost of the materials and the physical architecture. The field is specifically lacking in knowledge and understanding of the microbial community within the anode and cathode chamber, as well as bacterial electron transfer to a surface at a molecular level. For eventual optimization of MEC performance, the focus of investigations should be anode-associated communities and the different roles that various organisms play in current density, which indicates the power performance of the cell in A/m^2.

1.7. Scope of work

Currently there are still many unknowns in MEC research, specifically community dynamics within MECs, including which microorganisms function best at the anode and how these organisms transfer electrons. The scope of work was designed to address one of the key gaps in the literature, how the microbial community changes over time and their colonization strategy of

the electrode. Research carried out within the frame of this thesis to satisfy objectives listed in section 1.2. is described in the following chapters. Specifically, chapter 2 is a formal manuscript with this study's DGGE and homogenized FISH results. Chapter 3 describes the development of a biofilm embedding protocol for FISH to investigate community structure. Finally, chapter 4 will outline the conclusions and future work in this field.

CHAPTER 2: A TIME-RESOLVED ANALYSIS OF MICROBIAL ELECTROLYSIS CELL BIOFILMS

2.1. Introduction

Microbial electrochemical cells (MXCs), which include microbial fuel cells (MFCs) and microbial electrolysis cells (MECs), have become a well-studied alternative energy biotechnology in the last decade due to their potential to generate either electricity or biohydrogen. They have been shown to produce current using complex organic waste materials, including various types of wastewaters (Ahn and Logan, 2010; Rodrigo *et al.*, 2007) or cellulosic waste products (Rezaei *et al.*, 2009, Lalaurette *et al.*, 2010). They are considered a more environmentally friendly alternative energy source, because they are carbon neutral, releasing only recently fixed carbon back into the atmosphere (Lovley, 2006), and the biohydrogen produced has a variety of uses including bioremediation through redox reactions by reducing water pollutants, as well as the hydrogenation of many products, including gasoline and fertilizers (Lee *et al.*, 2010).

MXCs have been researched extensively by various research groups using a range of experimental setups (Logan, 2008; Rittmann, 2008). However, the main concepts remain similar. In general, MXC setups facilitate electron liberation from organic matter using anode-respiring bacteria (ARBs), microorganisms in the anode chamber of MXCs that oxidize substrates to generate electrons and other metabolic products (Lovely, 2006). The electrons yielded from the oxidation are passed into the anode and then transferred to cathode via an external circuit. In MEC's, a specific type of electrochemical system and the focus of this investigation, oxygen is removed from the cathode chamber and a small amount of external voltage is added in order to produce hydrogen gas at the cathode (Call and Logan, 2008). MECs were chosen for this investigation because of the many uses of their end product, biohydrogen.

Currently one of the major hurdles in practically implementing MECs is that the power densities produced are still too low for most applications (Debabov, 2008). Research to improve these systems has focused more on the engineering aspect of the setups. Thus far, improvements to system architecture have resulted in MEC power densities increasing by five to six orders of magnitude in the last decade (Logan and Regan, 2006). However, there has been less emphasis on the microbial communities members that produce the current (Gupta *et al.*, 2011; Logan, 2009; Du *et al.*, 2007; Logan *et al.*, 2006). Further improvements might be achieved by understanding and engineering the microbial ecology at the anode, and community characterization is a crucial starting point toward this objective.

Key members of the microbial community in MECs are anode-respiring bacteria (ARBs), which are associated with the anode and are able to transfer electrons from an electron donor to the anode (Torres *et al.*, 2010). Many of these microorganisms have been isolated from naturally colonized anodes, previously inoculated with various mixed communities; however, it has been shown that these strains generate low power densities when grown as pure cultures (Rabaey *et al.*, 2004; Zuo *et al.* 2008). For example, *Shewanella oneidensis* consistently produces power densities that are much lower than mixed culture communities in MFCs (Watson and Logan, 2010) and lower current densities when compared to mixed cultures in MECs (Hu *et al.*, 2008). A possible explanation is that the complex mixture of organics present in most of the commonly used substrates might require a diverse microbial community to oxidize the various components, since many ARBs can only utilize a limited range of these substrates. Non-ARB microorganisms, including fermenters, methanogens, and homo-acetogens, have also been found in anode-associated biofilms. However, the relationship between the microbial community members and how they contribute to electron flow is still not well understood (Parameswaran *et*

al., 2009). It is also still unclear in what order these microorganisms colonize the anode after inoculation and how this may affect current production.

The focus for this investigation was to determine the composition of microbial communities in an anode-associated biofilm obtained from a functioning H-type MEC run in batch mode and inoculated with anaerobic digested sludge. The overall biofilm structure and changes in community composition over time were studied in conjunction with energy production to understand microbial interactions within anode biofilms and how changes in the community might affect current output. The microbial composition of biofilms colonizing an anode not connected to a cathode (the negative control) was also examined to determine which community members do not donate electrons to the anode, but use the electrode as simply a surface to attach and grow on. This was done by employing a negative control, an unattached electrode present in the anode chamber.

2.2. Methods and Materials

MEC Reactor Setup

The MECs were set up and run at the Center for Environmental Biotechnology within the Biodesign Institute at Arizona State University, shown in Figure 2.1 a and b. The anode chambers in these MECs were inoculated with 2 mL of 1% solids thickened anaerobic digested sludge (comprised of bacteria and archaea for the treatment wastewater) and return activated sludge from the Mesa Northwest Wastewater Reclamation Plant. All MECs were run in a two-chamber, H-type setup with 325 mL each for the anode and the cathode compartments and an AMI 7001 anion exchange membrane (Membranes International, Glen Rock, NJ) between the anode and cathode compartments. The anode electrodes were four square graphite rods, each with a surface area of 12.1 cm^2. The anode was poised at a potential of -400 mV (vs) Ag/AgCl reference electrode, based on previous studies done at ASU (Torres et al, 2010; Parameswaran et al, 2009). Both the anode and cathode compartments contained the same medium, which consisted of a 42 mM Na_2HPO_4, 7.5 mM KH_2PO_4, 7.7 mM NH_4Cl, mineral media, 4 mM $Fe(II)Cl_2$ stock solution, and 18.6 mM $Na_2S.9H_2O$ stock solution. After media addition, 0.49 mL of 100% ethanol solution was added to the anode compartment to obtain 100 meq and the MECs were run in batch mode at room temperature for 10 days, at which point a 1 cm^3 piece of the anode was snapped off and stored at -20ºC until for analysis. After initial sampling, the MEC was operated under continuous flow with a hydraulic retention time (HRT) of 10 hrs for an additional 100 d. Biofilm samples were obtained at 46, 81 and 110 d for FISH microscopy and community analysis.

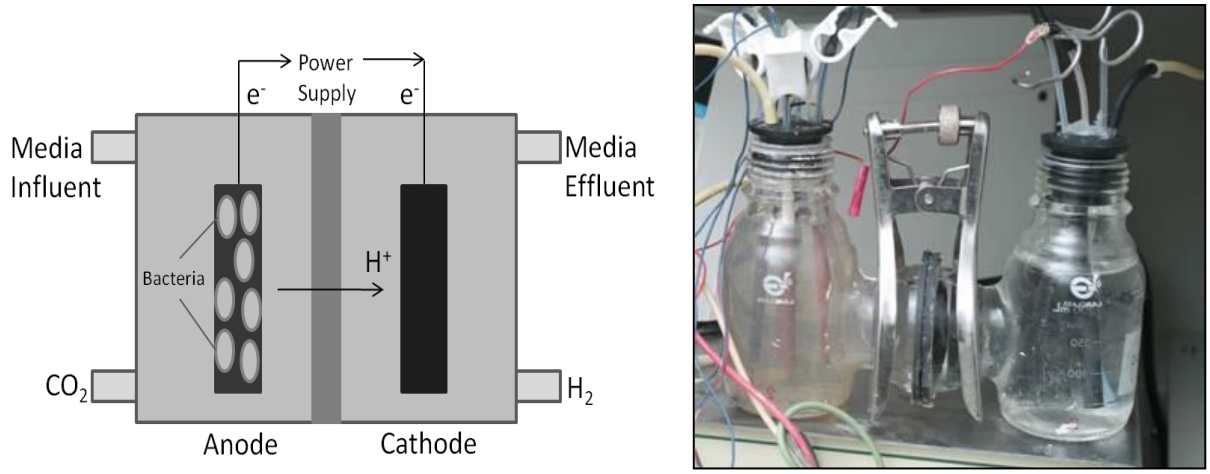

Fig. 2.1 a. Schematic of ethanol fed MEC b. Ethanol fed MEC with graphite electrodes, inoculated with anaerobic digested and waste activated sludge, and run at Arizona State University.

DNA Extraction and PCR Amplification

Electrode pieces were unthawed at room temperature and a biofilm sample on one side of the anode was removed from the electrode using a sterile scalpel. The biofilm DNA was extracted using a MoBio UltraClean Soil DNA Extraction Kit for environmental samples (MoBio Laboratories INC., Carlsbad, CA) following the manufacturer's instructions, followed by storage at -20°C. For each sample, two extractions were performed to minimize extraction bias.

Extracted and cleaned DNA was first unthawed at room temperature following storage at -20°C. Two sets of 16S rRNA bacterial primers and one set of archaeal 16S rRNA primers were used to amplify fragments of the 16S rRNA gene, all synthesized at The SickKids Centre for Applied Genomics (TCAG) synthesis facility. In the first bacterial set, the forward primer used was U341F-GC (5'-CCTACGGGAGGCAGCAG-3') which had a GC clamp attached (5'-GGCGGGGCGGGGGCACGGGGGGCGCGGCGGGCGGGGCGGGGG-3') at the 5' end (Muyzer *et al.*, 1993). The reverse primer in set 1 was U758R (5'-CTACCAGGGTATCTAATCC-3'). This set produced a 418-bp fragment corresponding to positions 341 to 758 in the *Escherichia coli* 16S rRNA sequence within the variable regions V3

and V4 (Rolleke *et al.*, 1996). The second set of 16S rRNA bacterial primers was F1-GC (5'-GAGTTTGATCCTGGCTCAG-3'), which also had a GC clamp attached to the 5' end and U519R (5'-GTATTACCGCGGCTGCTGG-3'), producing a fragment size of 518bp (Yeung *et al.*, 2011). Lastly, the archaeal primers used were ARC344F-GC (5'-CGCCCGCCGCGCCCCGCGCCCGTCCCGCCGCCCCCGCCCGACGGGG(C/T)GCAGCAG GCGCGA-3') and ARC9115R (5'- GTGCTCCCCCGCCAATTCCT-3') (Yeung *et al.*, 2011).

The 50 µL PCR reaction mixture contained 1 µL of template DNA, ddH_20, 25 pmol of both the forward and reverse primer, 10x BSA (New England BioLabs, Pickering, ON), 200 µM of each dNTP (New England BioLabs, Pickering, ON), 2.5 units of Taq polymerase (New England BioLabs, Pickering, ON) in 10X Taq buffer (100 mM Tris-HCl pH 9.0, 500 mM KCl, 15 mM $MgCl_2$) (New England BioLabs, Pickering, ON). The PCR protocol for all three sets of primers was as follows: a temperature of 96°C for 5 min and thermocycling at 94°C for 1 min, the annealing temperature was set to 65°C and was decreased by 1°C at every 1 min cycle for 20 cycles, and a 3 min elongation time at 72°C. Additional cycles (15-20) were performed with annealing temperatures of 55°C for bacterial primers and 50°C for archaea (Yeung *et al.*, 2010). Upon completion of the protocol, the samples were loaded into a 0.5% agarose gel with SYBR Safe DNA gel stain (Invitrogen, Burlington, ON), visualized using the Invitrogen Safe Imager 2.0 (Invitrogen Canada, Burlington, ON) and quantified using a serial dilution of a 100-bp molecular weight ladder (MBI Fermentas, Amherst, NY) to create a standard curve.

Each sample was amplified three separate times using the same PCR protocol to minimize PCR bias. The products were combined, cleaned using the IBI Gel/ PCR DNA Fragments Extraction Kit (IBI Scientific, Peosta, IA) , and concentrated, if necessary, using a Savant DNA110 speed

vacuum (Fisher Scientific Limited, Nepean, ON). Quantification was done again using an agarose gel and a MW marker.

Denaturing Gradient Gel Electrophoresis (DGGE)

All DGGE gels were 8% polyacrylamide with a denaturing gradient of 30-70% (7 M urea and 40% deionized formamide was considered to be 100% denaturant) and were cast using a gradient former (BioRad Laboratories, Mississauga, ON). Approximately 500 ng of the 16S rRNA product was loaded into each well of the DGGE gel. The gel was run in a DCode Universal Mutation Detection System (BioRad Laboratories, Mississauga, ON). Electrophoresis was run at a constant voltage of 80 V for 16 hrs at 60°C.

All gels were stained for 30 min in SYBR Gold (Invitrogen, Burlington, ON) with gentle agitation followed by brief de-staining in 1X TAE. The gel was imaged using a Gel Logic 1500 Imaging System (Kodak, Rochester, NY). Bands of interest were excised and placed into 25 µL of sterile ddH_20, followed by incubation at 4ºC fridge for 48 hrs before re-amplification.

Gel images were analyzed for profile similarity using GelCompar II (Applied Maths, Sint-Martens-Latem, Belgium) to generate dendrogram profiles. The genotypes were visually detected based on the presence or absence of bands in each lane. A band was defined as present if its peak intensity was at least 5% of the most intense band in the sample. Dendogram patterns were clustered by the Dice method (Yeung *et al.* 2011) using arithmetic average groupings with a similarity coefficient matrix.

Reamplification of DNA from Excised bands

Samples were re-amplified with the same set of primers used in original PCR for the DGGE gel but without the GC-clamp. One microlitre of eluted DNA was re-amplified with the bacterial primers as follows: an initial denaturation of 5 min at 96°C, followed by 30 cycles of 94°C for 1

min, 60°C for 30 sec, and 72°C for 1 min (Yeung *et al.*, 2011). For archaeal primers, the previously discussed archaeal PCR protocol was repeated.

DNA Sequencing and Phylogenetic Analysis

Reamplified PCR products were purified using the IBI Gel/ PCR DNA Fragments Extraction Kit (IBI Scientific, Peosta, IA), quantified and sent to the The SickKids Centre for sequencing using the Applied Biosystems SOLiD 3.0 System. DNA sequences were edited manually using the reverse and forward sequences to create a single, consensus sequence and correct falsely identified nucleotides using FINCH TV (Geospiza, Seattle, WA). The 5' and 3' ends were also trimmed to remove unreadable parts of the sequence in Chromas V2.01 (Technelysium, Tewantin, Australia). Cleaned, consensus sequences were checked for similarity against 16S rRNA sequences found in the NCBI Database using BLAST (http://blast.ncbi.nlm.nih.gov/Blast.cgi).

Phylogenetic and molecular evolutionary analyses were conducted using MEGAV5.05.

The closest known sequences, as well as the closest isolates, were included in further phylogenetic analyses. Alignment of the sequences was carried out using ClustalW (http://www.ebi.ac.uk/clustalw/).

Fluorescent *in situ* Hybridization on Homogenized MEC Samples

The fixation and FISH protocols used on homogenized biofilm samples, which were removed from the anode surface using a sterile scalpel, are based on protocols developed by Amann (1995) and Manz *et al.* (1992). All samples subjected to FISH were first fixed in 4% paraformaldehyde (PFA), pH 7.4, (Sigma Aldrich, Oakville, ON) in order to stop physiological activity, preserve proteins and nucleic acids, as well as permeabilize cells (Amann, 1995).

Samples were fixed for 2 hrs at room temperature, followed by three washes of 1x PBS. Pellets were stored at -20ºC in a 50:50 ratio of ethanol to PBS until further processing.

Samples were removed from storage and dried on gelatin/chromium potassium covered slides, followed by ethanol dehydration. Samples were then hybridized with oligonucleotide probes by placing slides in hybridization buffer (5 M NaCl, 1 M Tris-HCl, 10% SDS, formamide, and ddH_20) (Manz *et al.*, 1992) for 1.5 hrs at 46ºC with a maximum of 2 probes at a time. Probe combinations were either Cy5-ARC915 (5'–GTGCTCCCCCGCCAATTCCT-3') labeled with Cy5 to target all Archaea (Stahl and Amann, 1991) and Cy3-EUB338 (5-GCTGCCTCCCGTAGGAGT-3') labelled with Cy3 to target all Bacteria (Amann *et al.*, 1990), using 35% formamide or Cy5-ModSRB385 (5'-CGGCGTYGCTGCGTCAGG-3') labeled with Cy5 to target >2900 *Geobacter* species (Ren *et al.*, 2008) and Cy3-EUB338, using 30% formamide for hybridization. Probes were synthesized by IDT (Coralville, IA). After hybridization, the slides were submerged in a washing buffer (Manz *et al.*, 1992) (5 M NaCl, 1 M Tris-HCl, 10% SDS, 0.5 M EDTA and ddH_20) at 48ºC for 20 min, rinsed with ddH_20 and air dried prior to storage.

Visualization of hybridized cells was performed on a Zeiss LSM 510 Confocal Laser Scanning Microscope (Carl Zeiss Canada LTD., Toronto, ON) equipped with 3 lasers (488, 543, and 633 nm) and using the C-APOCHROMAT 63X/ 1.2 water corrective lens.

Images obtained from the CLSM were analyzed to determine the relative quantity of all *Bacteria*, *Archaea*, and *Geobacter* species using ImageJ V1.45i (http://rsbweb.nih.gov/ij/download.html). Images were split into their respective channels and a signal threshold was set manually prior to image binarization and determination of the percentage of area covered by FISH-mediated signals in each image. The relative abundance of

Archaea to *Bacteria*, was calculated and expressed in percentages of total cell signals. It was also determined what the relative abundance of >2900 *Geobacter* sp. to *Bacteria* was, and expressed in percentages of EUB338 signals. To determine if population changes were statistically significant in either of these two trials, a regression analysis was performed using SYSTAT V.13 (Systat Software Inc., Chicago, IL) with a p-value of 0.001 and the relative abundance values for 10 images.

2.3. Results

Current production in an ethanol fed MEC

After a lag period of about 4 days, the batch MEC started producing current (Fig. 2.2). Current density increased exponentially until it stabilized on day 10 at 2.0 A/m^2. Methane production was detected during the exponential growth, although the gas volume could not be recorded. The coulombic efficiency also stabilized by the end of day 10 at 57.5% (data not shown), the end of the batch run. This was based on the addition of 26.4 mM (103 meq) ethanol at the beginning of batch mode and is comparable to previously reported values for ethanol fed MECs at ASU (Parameswaran *et al.*, 2009; Torres *et al.*, 2007).

Batch mode was complete once current density and coulombic efficiency stabilized and the reactor was subsequently run in continuous mode, with sampling performed at 46, 81, and 110 days of operation from the start of the MEC. An average steady state current density of around 6 A/m^2 was maintained for the first 20 days of continuous operation. However, around 20 days into continuous operation, problems of media contamination arose which was reflected by the drop in current density. Even after media replacement was completed, current densities dropped to 2.1 A/m^2 and never recovered to the previous values of 6 A/m^2 through 46 days (data not shown). Current density eventually increased to 7.0 A/m^2 at day 81. At the final point of sampling, day 110, current density reached 8.1 A/m^2. Also, it was noted that at day 10 the standard deviation for current density was larger (1.30), than the standard deviation for days 46, 81, and 110 (0.12, 0.18, and 0.06 respectively), as current density increased. Overall there was an increase in current density over time which stabilized. Stabilization was indicated by a decrease in the daily change of values, measured by taking the standard deviation of all current density values on each sampling day.

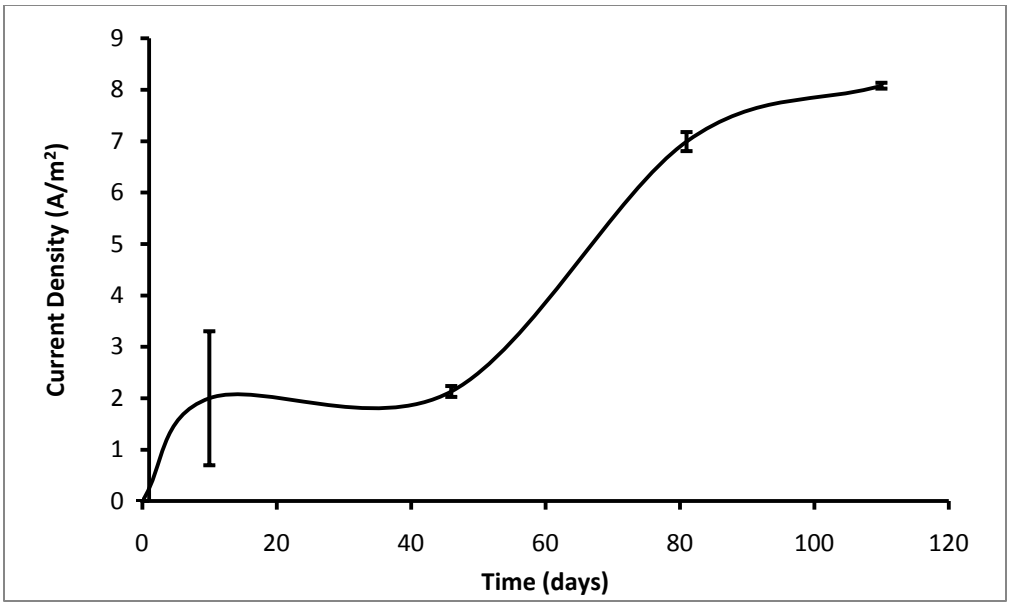

Fig 2.2. The current density produced in an ethanol fed MEC inoculated with anaerobic digested sludge. Current density is an average of the data points for the days on which samples were collected for DGGE and FISH analysis (day 0, 10, 46, 81, and 110). Error bars are standard deviation of the current density throughout the each day.

Bacterial DGGE Analysis

Cluster analysis of bacterial 16S rRNA gene fragments was performed using the bacterial dendogram in Fig. 2.3. This was done in order to analyze changes in the MEC microbial community over the 110 days runtime; samples from the MEC reactor were collected at days 0 (inoculum), 10, 46, 81 and 110, as well as from the negative control (unattached electrode) and suspension from day 110.

Cluster analysis of the bacterial DGGE revealed a low S_{AB} value (Similarity Index) between the inoculum and all subsequent samples with 41.0%. As well, the day 10 sample showed a high amount of dissimilarity to the rest of the samples with an S_{AB} value of 66.2%, as well as compared to the inoculum (49.8%). The other five samples had more similar banding patterns, especially the days 46 and 81 (96.8%) which clustered with day 110 (76.5%), while the reactor

control sample (electrode not connected) and the anodic chamber suspension sample, obtained on day 110 clustered with a S_{AB} value of 76.5%.

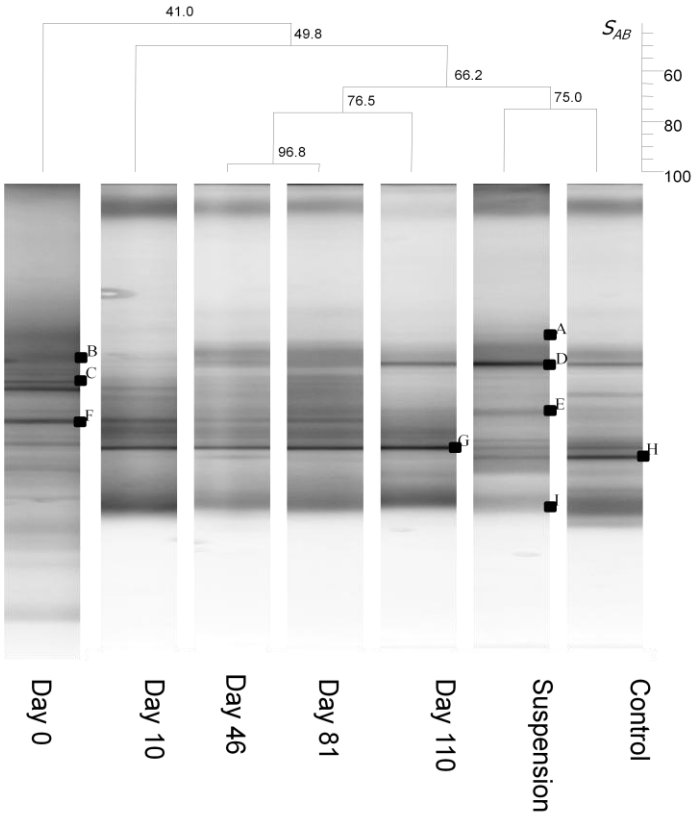

Fig. 2.3. Dendrogram of bacterial DGGE with cluster analysis of banding patterns. Bands collected for sequencing are marked with letters (A-I) for all 7 samples (day 0 (inoculum), 10, 46, 81, and 110) from an ethanol fed MEC.

Specific phylogenetic information was determined by sequencing distinct bands from the bacterial DGGE gel (shown in the dendogram in Fig. 2.3). Nine unique sequences from the bacterial DGGE were established after blasting the results (Table 2.1). It was also noted in figure 2.3, the appearance and disappearance of certain bands. Specifically of note is the late appearance of *Pelobacter* (Band D) and *Dysgonomonas* (Band A), as well as the early disappearance of *Clostridium* (Band C).

Table 2.1. Closest GenBank matches and isolates of sequences obtained from the bacterial DGGE in Fig. 2.3.

Name	Closest Match	%	Closest Isolate	%	Phylum
A	Uncultured *Dysgonomonas* sp. clone MFC63F06 16S ribosomal RNA gene, partial sequence	90	*Dysgonomonas gadei* partial 16S rRNA gene, clone MFC-EB6	90	Bacteriodetes
B	Uncultured bacterium clone PS7 16S ribosomal RNA gene	94	*Bacteroidales bacterium* 33bM 16S ribosomal RNA gene, partial sequence	93	Bacteriodetes
C	Uncultured bacterium clone MEC9-26 16S ribosomal RNA gene, partial sequence	93	*Clostridium* sp. 6-44 gene for 16S ribosomal RNA, partial sequence	88	Firmicutes
D	Uncultured bacterium partial 16S rRNA gene, isolate DGGE band 9_cons6-2	99	*Pelobactrer acetylenicus* 16S rRNA	97	Deltaproteobacteria
E	Uncultured bacterium clone 72c 16S ribosomal RNA gene, partial sequence	98	*Wolinella succinogenes* strain ATCC 29543 16S ribosomal RNA, partial sequence	98	Epsilonproteobacteria
F	Uncultured bacterium clone potato_MFC40 16S ribosomal RNA gene, partial sequence	98	*Geobacter* sp. T32 16S ribosomal RNA gene, partial sequence	98	Deltaproteobacteria
G	Uncultured *Geobacter* sp. clone NS1 16S ribosomal RNA gene, partial sequence	98	*Geobacter sulfurreducens* KN400, complete genome	98	Deltaproteobacteria
H	Uncultured bacterium clone potato_MFC40 16S ribosomal RNA gene, partial sequence	99	*Geobacter* sp. T32 16S ribosomal RNA gene, partial sequence	99	Deltaproteobacteria
I	Uncultured *Desulfuromonas* sp. isolate DGGE gel band A-15-13-11 16S ribosomal RNA gene, partial sequence	97	*Pelobactrer acetylenicus* 16S rRNA	97	Deltaproteobacteria

Most of the sequences showed at least a 97% match to available sequences in GenBank, however, all were uncultured bacteria. It was revealed that the closest known isolates of all bands did belong within phyla and subphyla of known MEC anode-associated microorganisms, specifically *Deltaproteobacteria*, *Epsilonproteobacteria*, *Bacteriodetes* and *Firmicutes* (Table 2.1). A phylogenetic tree was constructed based on the sequences obtained and is shown in Fig. 2.4.

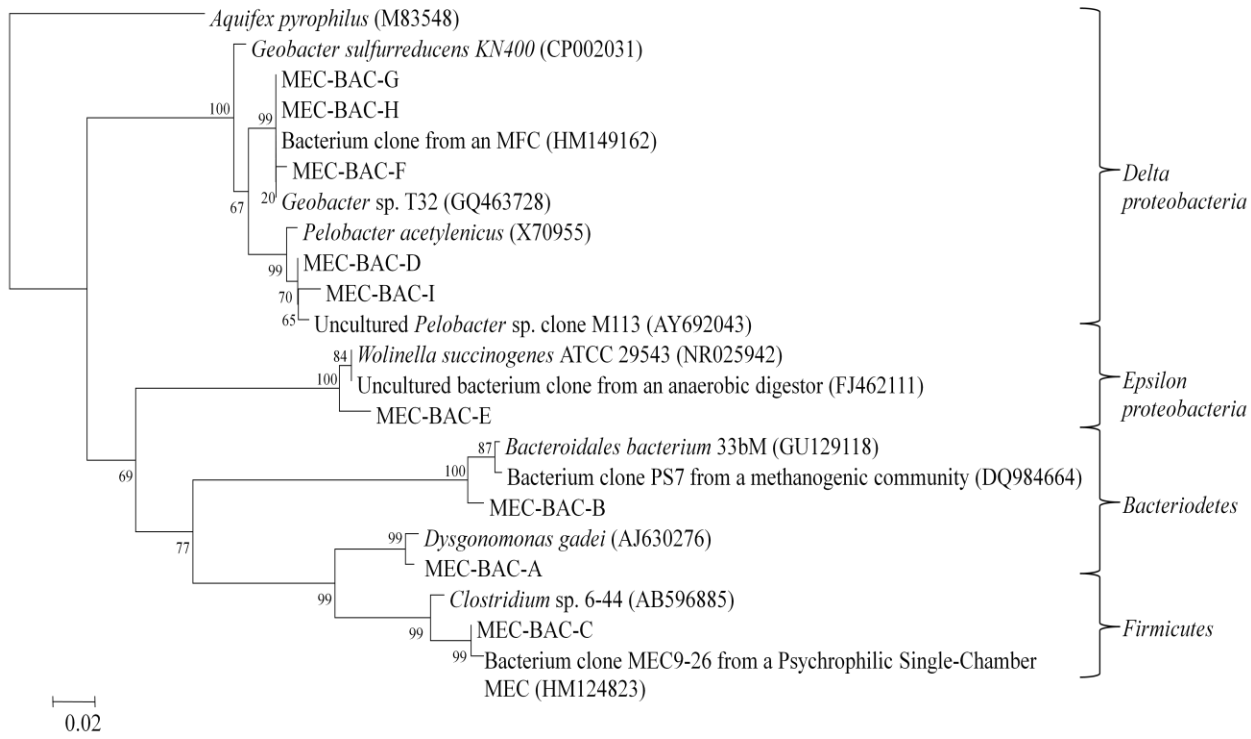

Fig. 2.4. Phylogenetic relationship of the 9 bacterial 16S rRNA gene fragment sequences obtained from microbial electrolysis cells over the course of the reactor runtime (110 days), including the suspension and negative control taken at day 110. The DGGE bands were assigned the label Microbial Electrolysis Cell-Bacteria (MEC-BAC) and their band letters are from Fig. 2.3. The tree was inferred by neighbour-joining analysis of the sequences obtained from DGGE. *Aquifex pyrophilus* was used as the outgroup. Numbers on the nodes are the bootstrap values based on 1000 replicates. The scale bar indicates the estimated number of base changes per nucleotide sequence position.

Archael DGGE Analysis

Archaeal phylogenetic information was determined by sequencing bands from the DGGE gel that was run with PCR products amplifiifed with archaeal 16S rRNA primers (Fig. 2.5). Three bands were excised and sequenced and all of them showed at least a 96% match to available sequences from GenBank.

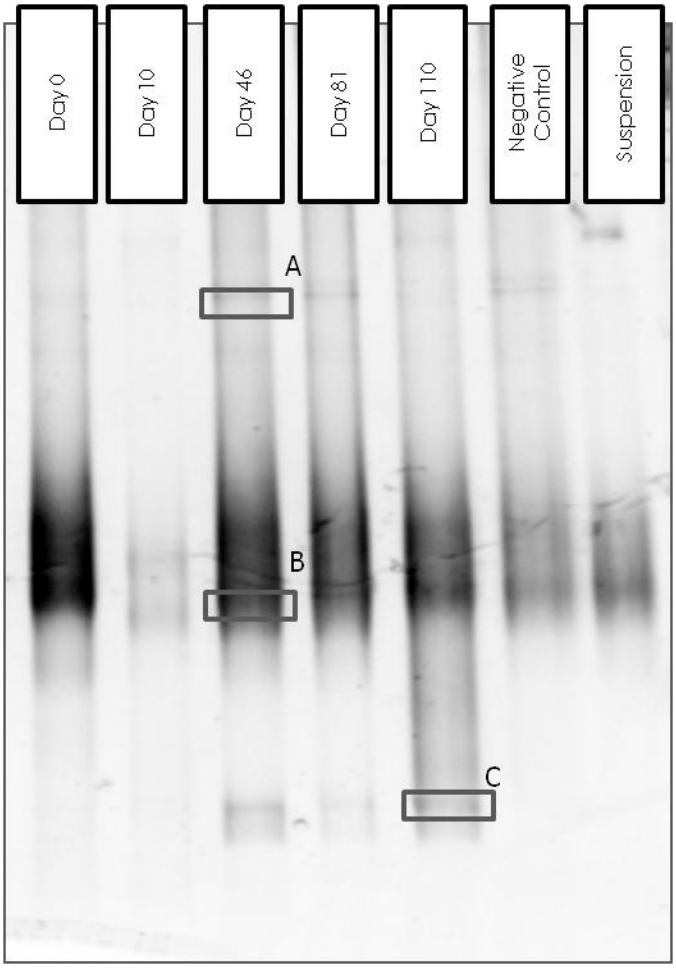

Fig. 2.5. DGGE gel of PCR products obtained with an archaeal primers amplifying the 16S rRNA region in *Archaea.* Samples were obtained from an ethanol fed H-type MEC inoculated with anaerobic digested sludge at days 0, 10, 46, 81, and 110 (including the suspension and a negative control electrode from day 110).

All three archaeal DGGE bands were within the phylum *Euryarchaeota* and are closely related to known hydrogenotrophic methanogens. Two of the three bands were related to *Methanobacterium* species, while the third was closely associated with *Methanobrevibacter alcaliphilum* (Fig. 2.6). No dendogram was produced from the archaeal DGGE, as only a few bands were revealed for each sampling time. The archaeal DGGE from different sampling time all revealed the presence of methanogens.

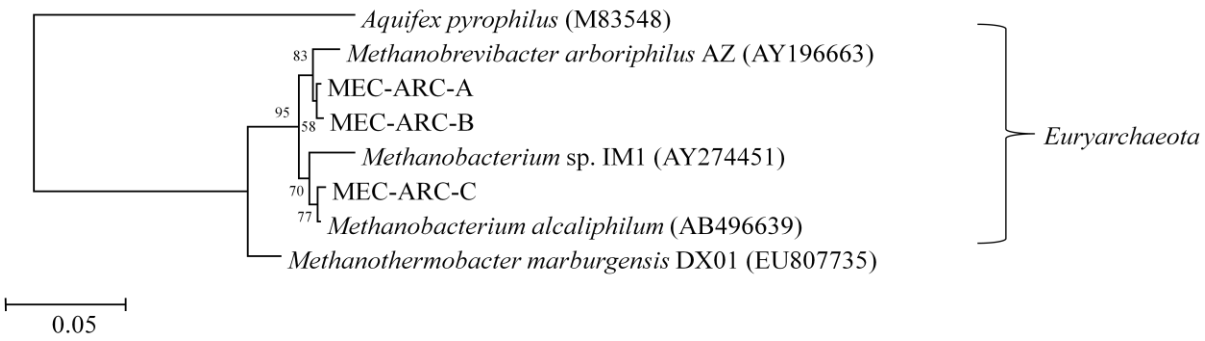

Fig. 2.6. Phylogenetic relationship of the 3 archaeal 16S rRNA gene sequences obtained from microbial electrolysis cells over the course of the reactor runtime (110 days), including the suspension and negative control taken at day 110. The bands were labelled with Microbial Electrolysis Cell-Archaea (MEC-ARC) and their band letters are from Fig. 6.16. The tree was inferred by neighbour-joining analysis of the sequences obtained from DGGE. *Aquifex pyrophilus* was used as the outgroup. Numbers on the nodes are the bootstrap values based on 1000 replicates. The scale bar indicates the estimated number of base changes per nucleotide sequence position.

Relative Abundance of *Bacteria* to *Archaea*

Bacteria and *Archaea* were detected using FISH and domain-specific probes hybridized to homogenized biofilm samples. To determine how the relative quantity of both groups were changing throughout the reactor runtime (Fig. 2.7), using Image J, probe signals were expressed in percentages of total cell signals determined by whole-cell hybridisation, based on Fig.s 6.1.-6.7. (Appendix A).

The microbial communities analyzed were dominated by *Bacteria* (probe EUB338), whereas *Archaea* (probe ARC915) in all samples remained below 35% of total probe-hybridized cells. The highest amount of *Archaea* was found in samples that were not directly responsible for current production (the inoculum, negative control electrode, and suspension, with 33.0%, 34.6% and 33.9%, respectively). Between days 46 and 110 (corresponding to a simultaneous increase in current production, Fig. 2.2) *Archaea* ranged from 23.6% (day 46) to 16.4% (day 110) of total cells. Overall, *Archaea* decreased to just less than half the original value of 16.4% on day 110 from 33% in the inoculum (day 0), while *Bacteria* increased from 67% in the inoculum to 83.6% at day 110. This corresponded to an overall increase in current production over the runtime of the reactor (inoculum to day 110) of 8.l A/m^2. The overall decrease in *Archaea* within the community was determined to be statistically significant upon performing a regression analysis and using a p-value of 0.001.

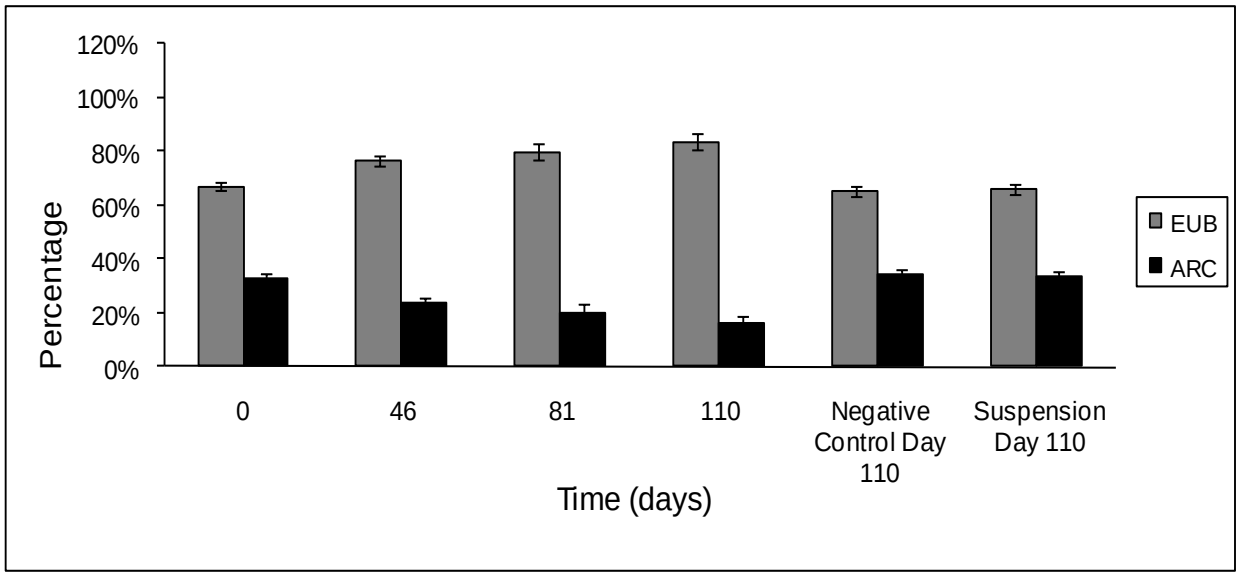

Fig. 2.7. Bar graph showing the relative abundance of Archaea, detected with the probe ARC915, and the relative abundance of Bacteria, detected using the probe EUB338, expressed in percentages of total cell signals determined by whole-cell hybridisation. Percentages were calculated at four sampling points for homogenized biofilm, as well as for a negative control

electrode (unattached electrode) and the anode suspension at day 110, from a microbial electrolysis cell inoculated with anaerobic digested sludge (day 0). Error bars indicate standard error. Values were calculated from Fig.s 6.1.-6.7. (Appendix A).

Quantity of *Geobacter* species within the overall bacterial community

The abundance of *Geobacter* species (probe ModSRB385) was measured relative to the abundance of *Bacteria* (probe EUB338) and expressed in percentages of EUB338 signals determined by whole-cell hybridisation (Fig. 2.8). The microbial communities analyzed were found to contain >60% *Geobacter* species of the entire community of *Bacteria* at all time points throughout the lifetime of the MEC reactor. Interestingly, the lowest percentage of *Geobacter* species was found in the unattached, negative control electrode at 62.1%, which served no purpose in the reactor other than as a colonization surface. The overall trend for electrode-attached biofilm samples was an increase in the percentage of detectable *Geobacter* spp., from 69.6% of total *Bacteria* in the inoculum to 93.3% at day 110. This change in the community also corresponds to a statistically significant increase in current production from inoculation to day 110 using a p-value of 0.001.

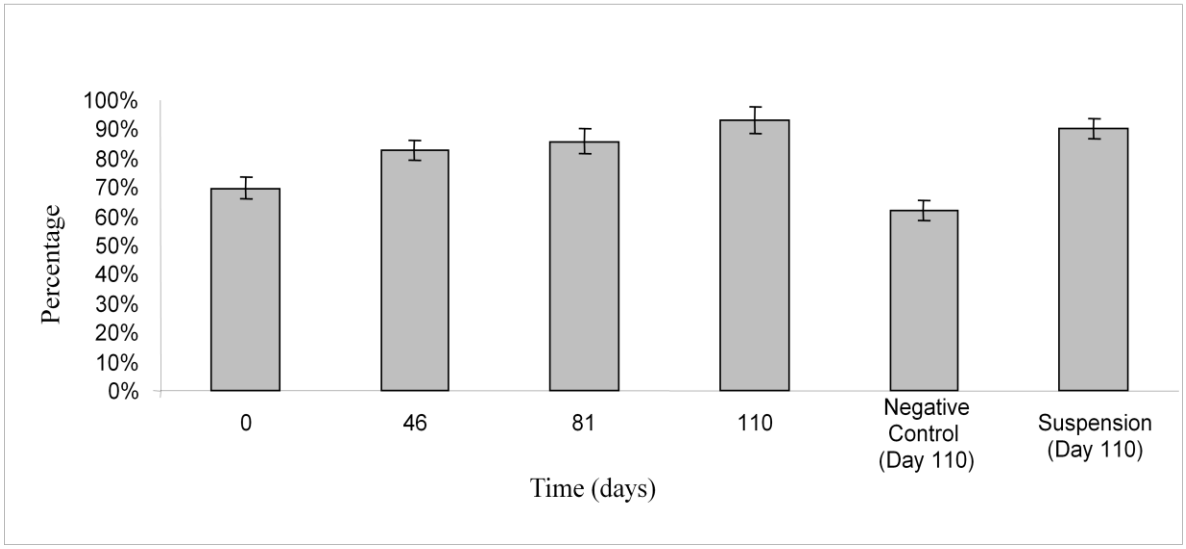

Fig. 2.8. Bar graph showing the relative abundance of Geobacter spp., detected using the probe ModSRB385, to the relative abundance of Bacteria, detected with the probe EUB338, expressed in percentages of EUB338 signals determined by whole-cell hybridisation. Percentages were calculated at four sampling points for homogenized biofilms, as well as for a negative control

electrode (unattached electrode) and the anode suspension at day 110, from a microbial electrolysis cell inoculated with anaerobic digested sludge. Error bars indicate standard error, where all values are <5%. Values were calculated from Fig.s 6.8.-6.13. (Appendix A).

2.4 Discussion

Numerous groups have looked at the 16S rRNA gene to investigate the microbial diversity in microbial electrolysis cells (Cusick *et al.*, 2010; Logan and Regan, 2006; Chae *et al.*, 2008; Parameswaran *et al.*, 2010); however, to our knowledge, only one group has actually performed a time-resolved analysis of an MXC microbial community (Aelterman *et al.*, 2006). Aelterman *et al.*'s conclusions indicated that without modifying the substrate or MFC configuration, there was an overall decrease in internal resistance and increase in current density over time. Consequently, this was attributed to intrinsic alterations of the anode-associated biofilm, specifically a shift from a more diverse microbial community in the inoculum to a more uniform community in the MEC, when there are less bands present (Fig. 6.16). Similarly, even though the sampling time points in our investigation were much earlier, cluster analysis (Fig. 2.3) performed on our bacterial DGGE gel revealed a low similarity index value (S_{AB}) between the inoculum and all other samples (41.0%), as well as the day 10 sample compared to all the other samples from subsequence time points, compared to much higher S_{AB} values later on between sampling times. Therefore the bacterial DGGE revealed a highly changing community from the original inoculum and day 10, to a more uniform community structure towards the end of the reactor runtime. Concurrently, there was an increase in current density as the S_{AB} increased with time. It is also interesting to note, the standard deviation for current density (Fig. 2.2) earlier on in the reactor runtime (day 10) is much higher than the later time points (46, 81, and 110), where standard deviation is very low (0.12, 0.18, and 0.06 respectively), while simultaneously current density is increasing. As well, current density both increases and stabilizes (based on a low standard deviation of current density production on those days) the most between days 46 and 81

(2.1 A/m^2 to 8.1 A/m^2) when there is the highest S_{AB} value is seen amongst samples (96.8%), further substantiating the concept that a more stable community results in a higher, more stable current and overall more efficient MEC. It is known that a microbial community is capable of establishing the properties of a biofilm and its features (Sutherland, 2001). As a result, the adaptation or change of the microbial community is probably having influence on the biofilm properties, specifically electrochemical properties in this case, and community stabilization promotes the production of current density (Reguera *et al.*, 2005).

Sequencing analysis based on this bacterial dendogram (Table 2.1) reveals further information on MEC community dynamics. It is expected that bands present on a DGGE gel constitutes at least 1% of the total microbial community (Muyzer *et al.* 1993). Therefore few DGGE bands in all lanes except the inoculum, indicates that the bacterial diversity is relatively low (Fig. 2.3). While the number of different community members seem to vary in MECs, the actual species seems to be relatively common, as eight of the nine unique bacterial DGGE bands were known members of microbial electrolysis cell communities when reactor conditions were similar (Parameswaran *et al.*, 2009), and even when they differed in inoculum, substrate or setup (Aelterman *et al.* 2006; Call *et al.*, 2009; Rabaey *et al.*, 2004, Fung *et al.*, 2006). Specifically the presence of *Deltaproteobacteria* (*Geobacter* and *Pelobacter* sp.), *Bacteriodetes* and *Firmicutes* (Table 2.1) is relatively common in mixed MEC communities. This implies that these organisms have a defined role in current production and if they are present in the inoculum, even with a low abundance, they will most likely survive and proliferate within the anode chamber when the conditions are favourable.

One of the most common species found in fuel cell communities is related to those within the family *Geobacteraceae*, known ARBs capable of consuming H_2 or acetate and transferring the

recovered electrons directly to the anode (Parameswaran *et al.*, 2010). *Geobacter* species, most commonly *G. sulfurreducens*, is common to most fuel cell mixed communities from different inoculum sources, and *Geobacter* species are well-defined in the role of anode respiration (Rabaey *et al.*, 2003; Jung and Regan, 2007; Lee *et al.*, 2008; Parameswaran *et al.*, 2010). Homogenized FISH data using the ModSRB385 probe, also indicated a high proportion of the bacterial community was *Geobacter*, seen by Parameswaran *et al.* (2011), when qPCR was used, as well and only increased over time from 69.6% of the total bacterial community at day 0 to 93.4% at day 110 (Fig. 2.8). This proliferation in *Geobacter* occurred in parallel with an increase in current density. With the well-defined role of *Geobacter* in fuel cell communities, it is unsurprising to see a simultaneous increase in anode respiration and current production pending there are microorganisms present to ferment the substrate, ethanol and in this community it was mostly likely *Pelobacter.*

Pelobacter is thought to be associated with ethanol fermentation rather than anode respiration, producing hydrogen to be further utilized downstream by other members of the community (Parameswaran *et al.*, 2010). This is supported by research showing that *Pelobacter carbinolicus* alone was not capable of anode respiration in an ethanol-fed MFC, but current generation was seen in a 50:50 mixture with *Geobacter sulfurreducens* (Richter *et al.*, 2007). It is also well documented that many species of *Pelobacter* (including *Pelobacter acetylinicus*, seen in this community) cannot reduce solid Fe(III), a mechanism common to *Geobacter* and other known ARBs (Schink, 1984).

The DGGE band closely related to a *Clostridium sp.* (*Firmicutes*) was found only within the inoculum and disappeared right after (Fig. 2.3). *Clostridium* species are known to ferment cellulose and other complex organics and within an ethanol-fed MEC, would have no substrate

to allow for proliferation. *Clostridium* species have been found to form synergistic relationships with *G. sulferreducens* at the anode and even become a dominant community member when the added substrate includes complex carbohydrates, such as wastewater (Kiely *et al.*, 2011). It would be beneficial to pursue further investigation of this organism for future MFC/MECs designed for wastewater treatment.

Lastly, species from the phylum *Bacteroidetes* have also been found by several other groups in anodal communities, specifically *Dysgonomonas sp*., also found in this study. Despite the fact that *Dysgonomonas* seem to be common on anodes, no strain has been shown to produce current in pure culture and based on the analysis in this investigation, it is still unclear what their roles in ethanol fermentation might be. However, its presence later on in the community is expected, as this is a slow growing organism (Holfstad *et al.*, 2000).

One genus not commonly found in MEC anodal communities is *Wolinella succinogens*, the only *Epsilonproteobacteria* found on day 110 after sequencing. A few groups have seen *Epsilonproteobacteria* in fuel cell communities; however their function has not yet been clearly indicated in the literature (Nielsen *et al.*, 2009; Parameswaran *et al.*, 2010). Parameswaran *et al.* (2010) did speculate that *Wolinella succinogenes* may be an ARB because it is very closely related to organisms within the genus *Campylobacter*, which contains species that are anaerobic and capable of utilizing acetate, H_2 gas, or formate as an electron donor (Logan, 1998). As well, they are unable to ferment simple alcohols, such as ethanol, the chosen substrate for this study (Penner, 1988). Recent unpublished research, utilizing a pure culture of *W. succinogenes* in the anode chamber of an H-type MEC, revealed that only very low current density was produced, supporting speculation that *W. succinogenes* could provide exogenous shuttles or help with direct electron transfer (Parameswaran, personal communication). The band did not appear until later in

microbial community and was also brightest and most distinct in the suspension, supporting the hypothesis that *Wolinella* is incapable of direct electron transfer.

In the archaeal DGGE gel (Fig. 2.5), only three bands were sequenced, and they are all closely related to known methanogens within the phylum *Euryarchaeota.* All three species are known to act as electron sinks in MECs since they are hydrogenotrophic methanogens, meaning they consume H_2 and convert it to methane. According to Chae *et al.* (2009) methanogenesis is one of the most critical causes of electron losses in MECs. Because acetate is a favourable substrate for methanogens, which converts it to methane and carbon dioxide, methanogens proliferate and create the largest electron sink in MECs if left uninhibited. In this reactor, methane was detected in the headspace but the quantity is unknown due to losses through the effluent. Several studies have reported that methanogens compete with ARB for the substrate, diverting electrons from the current production, and this becomes even more problematic with complex substrates (Call and Logan, 2008; Parameswaran *et al.*, 2009; Lee *et al.*, 2009). The FISH data in this study supports this hypothesis (Fig 2.7), since current density was lowest (2.0 A/m^2) when the presence of methanogens was highest (33%) and, as archaea continued to decrease throughout the lifetime of the reactor, current density increased. It is also notable that methanogens were still quite high at day 110 on the control (34.6%) and in the suspension (33.9%), indicating that they may have been partly 'driven off' the anode by ARBs. Although there was an overall decrease in the percentage of totals cells belonging to archaea, 16.4% of the electrode biofilm was still methanogens at day 110, most likely contributing to significant loss in electrons to methane.

Conclusions

Microbial electrolysis cells (MECs) are a promising source of biohydrogen for the future. However at present, current production within these units is too low to shoulder any of the

burdens of the world's increasing energy demands. In order to improve MEC function and allow for practical implementation, there needs to be a more clear understanding of the roles microorganisms play in current production, including further investigation into a method to inhibit methanogensis. This will allow for the capability to engineer an optimal current producing community and enhance overall hydrogen recovery in MEC systems.

CHAPTER 3: METHOD DEVELOPMENT: EMBEDDING PROTOCOL

3.1. Significance

Now knowing from the first part of this investigation that *Archaea* was present and acting as an electron sink, as well that *Geobacter* was in the MEC biofilm and contributed to increases in current density production, the next step was to find a way to investigate their spatial relationship. It was expected that the microorganisms directly associated with the electrode were most likely ARBs, probably *Geobacter*, and microorganisms associated with the peripheral edges of the biofilm were responsible for biofilm protection or electron scavenging.

In situ visualization and identification of microorganisms in complex environmental samples such as biofilms can be accomplished with the use of fluorescent *in situ* hybridization (FISH), a method which employs fluorescently labelled rRNA-targeted oligonucleotide probes to detect microorganisms with complimentary probe target sequences on their rRNA (Amann *et al.*, 1995). It is essential to embed the biofilm prior to hybridization in a medium in order to preserve the three dimensional structure of the biofilm and thereby visualize the spatial distribution of microbial cells within a biofilm. This chapter summarizes the embedding protocols tested in this work, and discusses the advantages and disadvantages of each protocol tested.

Studies utilizing the application of FISH to microbial communities in homogenized biofilm samples already exist (Mehanna *et al.*, 2010; Ren *et al.*, 2007; Zhao *et al.*, 2010). Some research groups have performed FISH directly on the electrode, without any embedding medium (Kiely *et al.*, 2011; Jang *et al.*, 2010). In general, this approach is destructive, due to large amounts of the biofilm matrix dislodging from the electrode as a result of a number of buffer changes (Amann *et al.* 1995). At present, some research groups have had success performing FISH on embedded samples, however such samples did not exist on a solid surface, like an electrode, but rather were

planktonic cells or tissues that could be easily thin sectioned after embedding (Bass *et al.*, 1997; Germroth *et al.*, 1995; Sato *et al.*, 1992). One group managed to publish well resolved embedded MEC images using a tissue embedding medium and cryosectioning (Chung and Okabe, 2009). The problem with this technique is that cryosectioning is difficult to do and often results in poor cellular morphology (Chen *et al.*, 2010).

The main objective in this part of the study was to develop a fast, easy to use embedding protocol for the application of FISH to intact, MEC-associated biofilms. The hybridized biofilms could then be viewed with a confocal microscope.

The development of such a protocol is also relevant for other areas of biofilm research where spatial distribution of microorganisms or microbial persistence on surfaces is being studied. More specifically it could be utilized in hospital settings, including studying colonization of equipment prone to contamination, such as catheters, or anaerobic cellulolytic communities where microorganisms form a biofilm on the cellulosic substrate. Overall, such a protocol will allow for the investigation of surface colonization and spatial interactions of microorganisms within biofilms in their *in situ* state.

3.2. Embedding in Polyacrylamide

Using polyacrylamide to preserve the spatial structure of MEC biofilms was initially proposed after a preliminary literature review (Germroth *et al.*, 1995; Hausen and Dreyer, 1981) to investigate commonly used embedding media. Christensen *et al.* proposed that polyacrylamide was effective because it is nonfluorescent, transparent and it solidifies at room temperature (Christensen *et al.*, 1999). This method has been used by other groups mostly successfully, to examine eukaryotic tissue cultures, cells, or cellular components, where samples were embedded in small wells of acrylamide (Bass *et al.*, 1997; Jiang *et al.*, 2006; Wang *et al.*, 2006). A similar

approach has also been used in small diameter tubing, where biofilms grow in a flow cell setup and polyacrylamide is pumped through the tubing at a slow flow rate and then left to solidify (Christensen *et al.*, 1999; Moller *et al.*, 1997). To my knowledge, no one has previously attempted to embed biofilm associated with MEC or MFC electrodes, or for that matter, any biofilm attached to a large, inflexible surface, in polyacrylamide for staining or FISH.

3.2.1. Polyacrylamide Embedding Protocol

Electrode pieces (1 cm x 1 cm) with attached biofilms were first fixed in 4% paraformaldehyde (PFA), pH 7.4, (Sigma Aldrich, Oakville, ON) according to the protocol developed by Amann (1995) for 2 hrs at room temperature. The electrode pieces were then placed into Petri dishes filled with 1 X PBS for 15 min, and transferred to fresh PBS for another 15 *min*. To prevent any unnecessary destruction or sloughing off of the biofilm during storage, samples were embedded immediately following fixation and washing.

The embedding protocol was based on the Christensen *et al.* (1999) protocol for embedding biofilms in silicon tubing, where 20% (w/v) acrylamide monomer is combined with *N,N,N',N'*-tetramethylethylenediamine (TEMED) and 1% (w/v) ammonium persulfate (APS) for the embedding medium. The embedding medium components were combined quickly and electrode pieces were placed in the solution within 3-5 min of mixing, as described by Christensen *et al.* The electrode was placed into a small Petri dish, covered with the acrylamide solution and left to solidify for 1 hr at room temperature. After solidification, the block of polyacrylamide containing the electrode piece was excised approximately 5 mm from the electrode edge and FISH was performed according to Amann (1995) and Manz *et al.* (1992). A hybridization time of 2 hrs and washing time of 30 min was used. The protocol was tested with only the EUB338 probe (5-GCTGCCTCCCGTAGGAGT-3') with a Cy5 label attached to avoid the use of

formamide and probe specificity related problems (Amann *et al.*, 1990). Once the final washing step was complete, the polyacrylamide block was gently rinsed in ddH_20 and placed onto a glass slide for visualization of hybridized cells using a Zeiss LSM 510 Confocal Laser Scanning Microscope (Carl Zeiss Canada LTD., Toronto, ON) and the A-Plan 10X/0.25 PH1 and LD-Achroplan 40X/0.6 corr Ph2 lens.

3.2.2. Results and Discussion

The first complication with this protocol was the time-sensitivity. This was noted by several authors who employed polyacrylamide as an embedding medium (Christensen *et al.*, 1999; Moller *et al.*, 1997). It was difficult to work so quickly with samples due to the quick polymerization time because samples have to be handled very delicately to prevent biofilm disruption.

If success was achieved in properly embedding the electrode piece in polyacrylamide, a block containing the sample was then excised with a scalpel. This was difficult, as it resulted in a slightly jagged cutting surface. It was also difficult to get very close to the surface of the electrode without hitting the biofilm or causing the polyacrylamide to detach. Because of this, there tended to be a thicker than desired layer around the electrode. This was most likely the main cause for the resulting images discussed below.

The images obtained from confocal microscopy revealed low resolution of the samples, shown in Fig. 3.1. a and b. All images exhibited diffuse cell signal. This was most likely the result of the polyacrylamide block surrounding the electrode being too thick and preventing sufficient diffusion of the probe to the biofilm surface. However, because the results did show some cell shape, especially in Fig. 3.1. a., it was suggested that perhaps the protocol could be modified to

improve results and sharpen images, using a non-toxic toxic medium with similar properties, agarose, discussed in section 3.4.

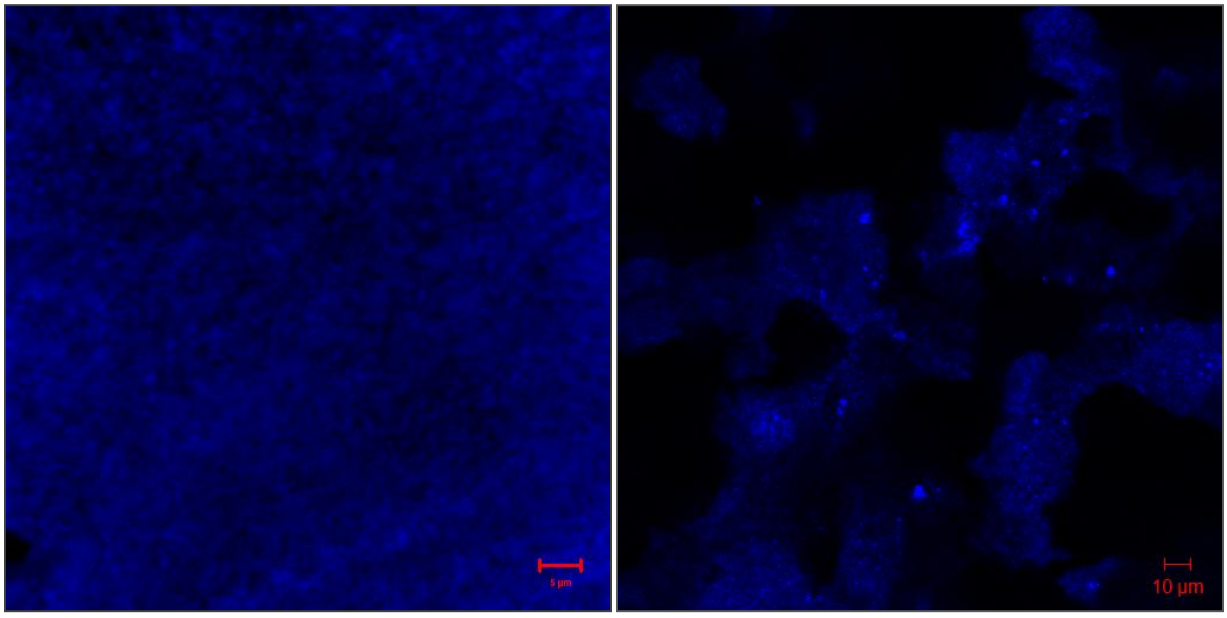

Fig. 3.1. a and b. Day 46 electrode piece embedded in polyacrylamide and hybridized to EUB338 (blue), targeting most bacteria.

3.3. Embedding in London Resin White

London Resin (LR) White is a hydrophilic, acrylic resin used as an embedding medium to preserve the structural state of a sample during various analytic techniques (Gros and Maurin, 2008). It polymerizes using a free radical mechanism, requiring the absence of oxygen during polymerization (Bowling and Vaughn, 2008). Previously, LR White has been successfully used in cases where probes or antibodies were used to visualize small scale eukaryotic samples (Nussbaumer *et al.*, 2006; Gros and Maurin, 2008). It was chosen as an embedding medium for its ease of use, the ability to ultrathin section the final, polymerized block, and its beam stability (Newman *et al.*, 1982). Because of the rigidity of the final polymerized block, it was decided that LR White might be a good candidate to maintain the structural integrity of anode-associated biofilms throughout the FISH protocol.

3.3.1. London Resin White Embedding Protocol

The protocol for embedding electrode pieces in LR White for FISH was derived from a procedure by Nussbaumer *et al.* (2006), where sections of hydrothermal vent tubeworms were embedded and thick sectioned to investigate the spatial organization of microbial endosymbionts. Samples were first fixed in 4% PFA, as described above in section 3.2.1., followed by dehydration in 100% ethanol for in 3 x 20 min. Electrode pieces were then transferred into 100% LR White resin (SPI Supplies, Westchester, PA) and put through 8 changes of resin at room temperature. Each resin change was 30 min. The samples were then transferred once more into fresh resin overnight to remove any excess ethanol. Resin polymerization required one final resin change, which occurred in 15 mL polyethylene tubes within a hybridization oven at 50° C for 48 hr. Unlike the Nussbaumer *et al.* (2006) protocol, our samples were not polymerized into gelatin capsules due to the size of the electrode pieces, which were too large for the diameter of available 13 mm gelatin capsules, and would have scraped the sides of the electrode when it was inserted.

In our case, polymerized samples could not be sectioned with a microtome, unlike similar LR White embedding protocols (Leitch *et al.*, 1990; Friedrich *et al.*, 1999; Nussbaumer *et al.*, 2006; Gros and Maurin, 2008), because the microtome would not slice through the graphite electrode. Instead, polymerized blocks of LR White containing the sample were notched with a jeweller's saw and then snapped. Alternatively, embedded samples were cut with a circular electrical saw. FISH was carried out on the two half blocks of LR White according to Amann (1995) and Manz *et al.* (1992). A hybridization time of 4 hrs and washing time of 30 min was used with LR White (Nussbaumer *et al.*, 2006), again using only the EUB338 probe (5-GCTGCCTCCCGTAGGAGT-3') with a Cy5 label (Amann *et al.*, 1990). Once washing was complete the embedding blocks were gently rinsed in ddH_20 and placed onto a glass slide for

visualization using a Zeiss LSM 510 Confocal Laser Scanning Microscope (Carl Zeiss Canada LTD., Toronto, ON) with the A-Plan 10X/0.25 PH1 and LD-Achroplan 40X/0.6 corr Ph2 lens'.

3.3.2. Results and Discussion

The first constraint encountered when using this protocol was that it was not possible to section the electrode with a microtome. The pieces that were used for FISH can be seen in Fig. 3.2. a and b. The surfaces resulting from either the snapping or cutting approach viewed under the microscope was uneven. Consequently, this resulted in only having small slivers of the focal plane in focus at one time, making it impossible to view the entire surface of the biofilm in one image. Our group was unable to derive a different protocol that would allow for this without disrupting the biofilm at the point of cutting or embedding.

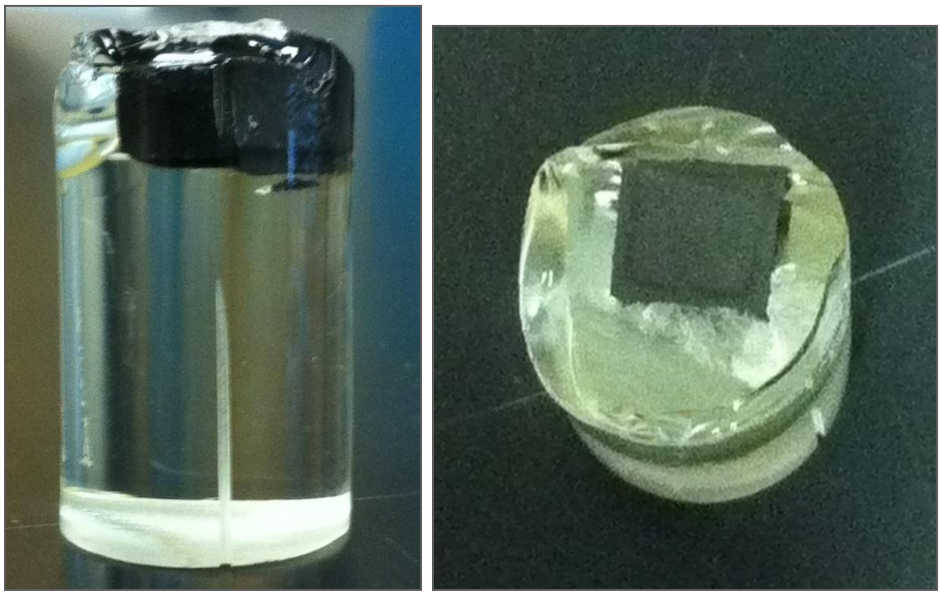

Fig. 3.2. a. The side profile of half an electrode piece embedded in LR White after snapping. b. Aerial view of an electrode piece embedded in LR White after snapping.

The inability to produce several sections of the sample also limited the number of surfaces available for hybridization to two areas, the surface at each point of snapping or cutting. This resulted in a bias, since only the microorganisms at the site of snapping could be seen, limiting

the reliability of the results and preventing proper statistical analysis with such a small sample size.

It was also determined, while carrying out the protocol, that this method would unlikely be suitable for our applications, due to the number of resin changes. Ten resin changes in total over the course of 24 hrs were required, among other liquid changes (i.e. ethanol) before polymerization occurred, in order to remove oxygen from the preparation. This was problematic because it was noted that as the resin changes occurred, small pieces of biofilm were detaching from the electrode. It was a concern that by the final step, a significant amount of biofilm was missing from the original state within the reactor, resulting in inaccurate conclusions.

Finally, when the two pieces were hybridized, the results did not give clear signals or show distinct cellular structure. Fig. 3.3 shows two images of the electrode surface, right at the interface of the electrode edge and LR White. Both images show the outline of the biofilm of the surface edge but the cell signal is diffuse, and it was difficult to distinguish any cell shapes. This may because, with such a large block of LR White, it was hard to remove all excess, unbound probe.

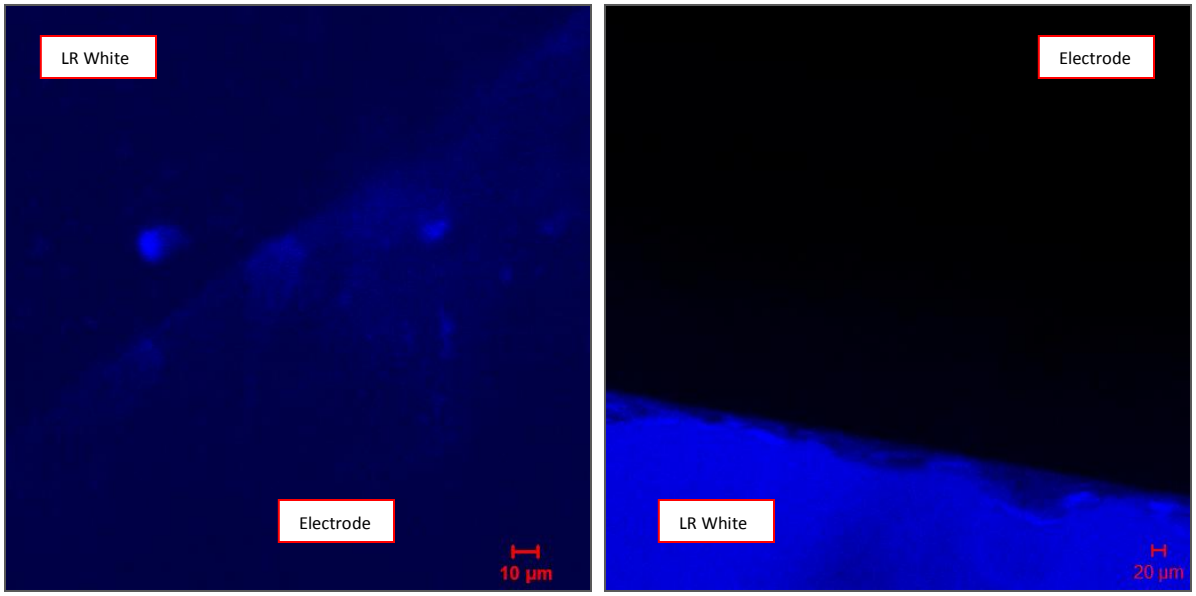

Fig. 3.3. a and b. Day 81 electrode pieces embedded in LR White and hybridized to the FISH probe EUB338 (blue), targeting most bacteria.

3.4. Embedding in Agarose

As mentioned in section 3.2.2, agarose was chosen based on the results observed using polyacrylamide as an embedding medium. It was proposed that these results could be improved, while working with a non-toxic alterative, agarose. The concept for this protocol was also based on the results of a few groups that performed catalyzed reporter deposition (CARD) FISH on polycarbonate filters embedded in agarose with success (Eickhorst and Tippkotter, 2008; Pernthalar *et al.*, 2002). Similarly to our work, the decision cited by the authors to embed filters was based on the large cell loss noticed after enzymatic treatment in the CARD-FISH protocol. It was noted that embedding in agarose prevented major cell loss due to cell lysis and detachment (Pernthalar *et al.*, 2002), as was also observed with our biofilm samples, when not embedded.

3.4.1. Test Protocol for Agarose Embedding Using Cells Deposited onto Glass Cover Slides

In order to proceed with the testing of embedding protocols, test pieces were generated by heat fixing 4% PFA-fixed *Escherichia coli* onto small pieces (approximately 1 cm x 2 cm) of glass cover slides. This was done by pipetting 10 µl of PFA-fixed *E.coli* onto cover slides and placing

them in a 60ºC incubator for 10 min. Slides were then removed from the oven and subjected to one of two conditions, ethanol dehydration or they were left unaltered until embedding. This was done to test the importance of ethanol dehydration prior to FISH and to determine whether is could be eliminated from the final protocol, since dehydration can cause extra biofilm sloughing. Both hydrated and dehydrated samples were embedded in 0.7% and 0.8% agarose (EMD Chemicals, Mississauga, ON) made with ddH_20. Both concentrations were tested to examine permeability of probes through the agarose matrix.

The agarose was made by heating the agarose and water in a beaker until the solution was boiling. Agarose was then poured into a Petri dish, and when the solution was cooled and on the verge of solidification, the cover slide pieces were placed in agarose and allowed to solidify completely for 1 hr at room temperature (Eickhorst and Tippkotter, 2008). Solidified agarose blocks containing cover slides were then excised with a scalpel and hybridized to only Cy5-labelled EUB338, as described by Amann (1995) and Manz *et al.* (1992). A hybridization time of 2 hrs and washing time of 30 min was used (Eickhorst and Tippkotter, 2008). Prior to visualization, samples were gently rinsed in ddH_20 and placed onto a glass slide for visualization. A Zeiss LSM 510 Confocal Laser Scanning Microscope (Carl Zeiss Canada LTD., Toronto, ON) was used with A-Plan 10X/0.25 and LD-Achroplan 40X/0.6 lens.

3.4.2. Final Protocol for Agarose Embedding of Electrode Surface-Associated Biofilms

The results of the first attempt to embed samples in agarose can be seen in section 3.4.3. Because they essentially appeared to be very similar to embedding in polyacrylamide and overall unsatisfactory, a new approach to embedding in agarose was attempted. It was also noted from the first attempt, that hydrated and dehydrated samples produced similar images, indicating that

dehydration was unnecessary, thereby eliminating three liquid changes in the protocol that might result in biofilm detachment.

The main objective in this attempt was to reduce the amount of agarose surrounding the sample pieces, so that the thickness of the agarose did not interfere with the available maximum working distance of 4.2 mm (using the A-Plan 10X/0.25 objective).

Test samples were generated using the same method as 3.4.1., using PFA-fixed *E. coli* and coverslips. The samples were removed from the oven and unaltered prior to embedding. 0.8% agarose was prepared in the same manner as described in section 3.4.1. and cooled until almost solidifying. At this point, sample pieces were placed on squares of parafilm and 20 – 30 µL of agarose was pipetted in a thin layer on one side of the cover slide. The agarose was left to dry for approximately 2 min before being turned over. Fresh agarose was then applied the other side, along with the edges to join the two sides of agarose and prevent them from slipping off. The fully embedded samples were left to dry at room temperature for approximately 1 hr prior to further treatment. FISH was performed in the same manner as the protocol described in the first attempt at agarose embedding, section 3.4.1. This included using Cy5-labelled EUB338, with a 2 hr hybridization period, followed by 30 min in washing buffer. Samples were visualized immediately following washing, before agarose pieces began to dry out using the Zeiss LSM 510 Confocal Laser Scanning Microscope (Carl Zeiss Canada LTD., Toronto, ON) was and the A-Plan 10X/0.25 Ph1 lens.

Following the success of this protocol with coverslip samples, the protocol was applied to MEC electrode pieces with attached anodal biofilm. The protocol was carried out the exact same way as it is described above using only Cy5-labelled EUB338.

3.4.3. Results and Discussion

In the first attempt at agarose embedding, the resulting images were very similar to those seen after embedding with polyacrylamide. Overall, cell structure was not very distinct, as shown in Fig. 3.4. a and b. In this attempt as well, excising the agarose block resulted in an uneven surface with a small focal plane when using the CLSM, more evident in Fig. 3.4. a, where the center of the image is in focus, while the periphery is out of focus. It was also difficult to cut through the agarose without disrupting the agarose and the scalpel blade proved not to be delicate enough for the task. Overall, results were promising but still left room for improvement.

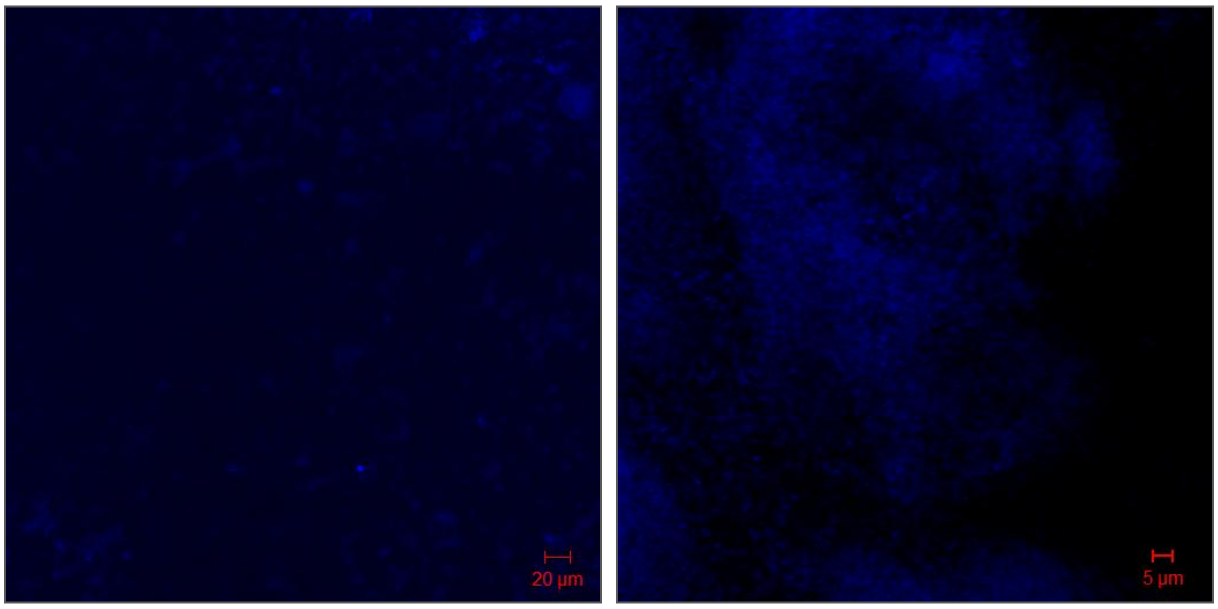

Fig. 3.4. a and b. Coverslips with heat fixed *Escherichia coli* embedded in 0.8% agarose and hybridized to the FISH probe EUB338 (blue) targeting most bacteria.

It was also in noted while experimenting with this protocol that samples did not need to be dehydrated in ethanol. The images obtained from sample pieces dehydrated looked very similar to those that were not, shown in Fig. 3.5 a, where the sample piece was dehydrated, and Fig. 3.5 b, where this sample was not. This indicated that dehydration could be removed from the protocol without consequence, thus eliminating extra liquid changes and unnecessary biofilm detachment.

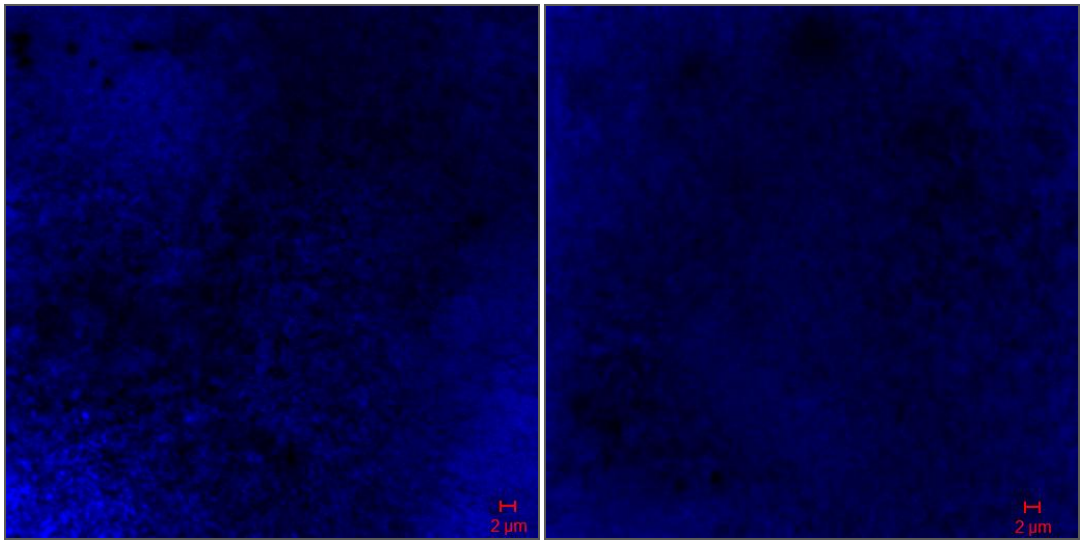

Fig. 3.5. a. *Escherichia coli* heat fixed on a coverslip, dehydrated in ethanol, hybridized to EUB338 and embedded in agarose. b. The same conditions as a. except without dehydration in ethanol.

The concentration of agarose used for embedding (specifically 0.7% and 0.8%) was also evaluated. It was important to use the lowest concentration of agarose possible to allow for maximum permeability of FISH probes. At the same time, the concentration of agarose had to be high enough to withstand the solution changes in the FISH protocol without washing off before visualization. With the difficulty of producing more electrode samples, since these anode-associated biofilms take weeks to grow in an MEC, it was important to have a protocol that would regularly function without problems. The 0.7% agarose regularly became detached by the washing step in the FISH protocol, while 0.8% agarose remained surrounding the biofilm and proved to be much more reliable. Therefore using 0.8% agarose to embed was permanently implemented into the protocol.

The second attempt at embedding biofilms in agarose now included the three major protocol changes that significantly improved the quality of the images produced, the removal of ethanol dehydration, embedding in 0.8% agarose, and applying only a very thin layer of agarose to the sample surface via pipette, eliminating the need for excision. The results from the protocol on

test pieces with *E. coli* are shown in Fig. 3.6. a and b. Following success with test pieces, the protocol was performed on an electrode piece from an MEC, shown in Fig. 3.7. a and b.

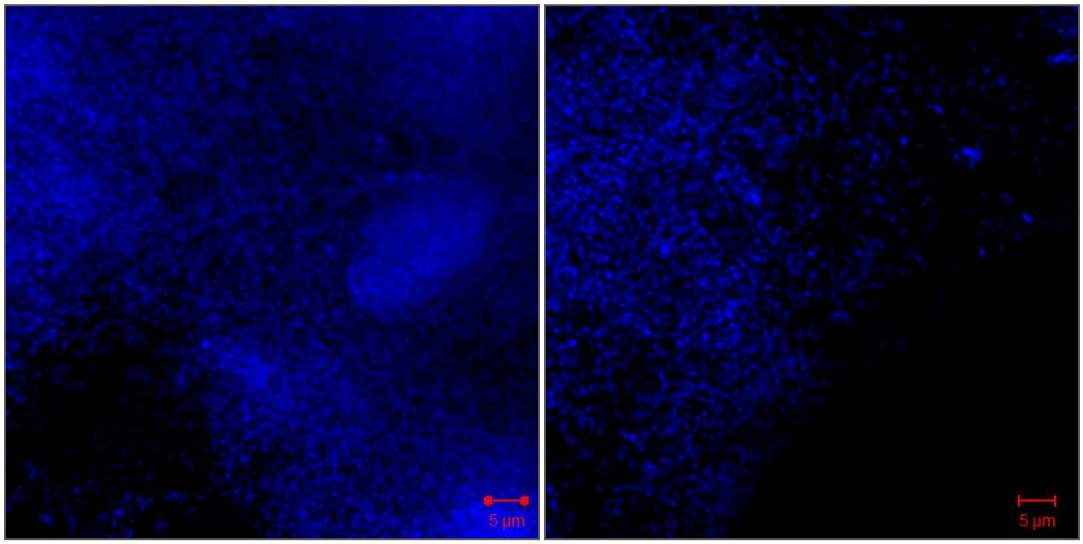

Fig. 3.6. a and b. *Escherichia coli* heat fixed on a coverslip hybridized to EUB338 and embedded in a thin layer of agarose.

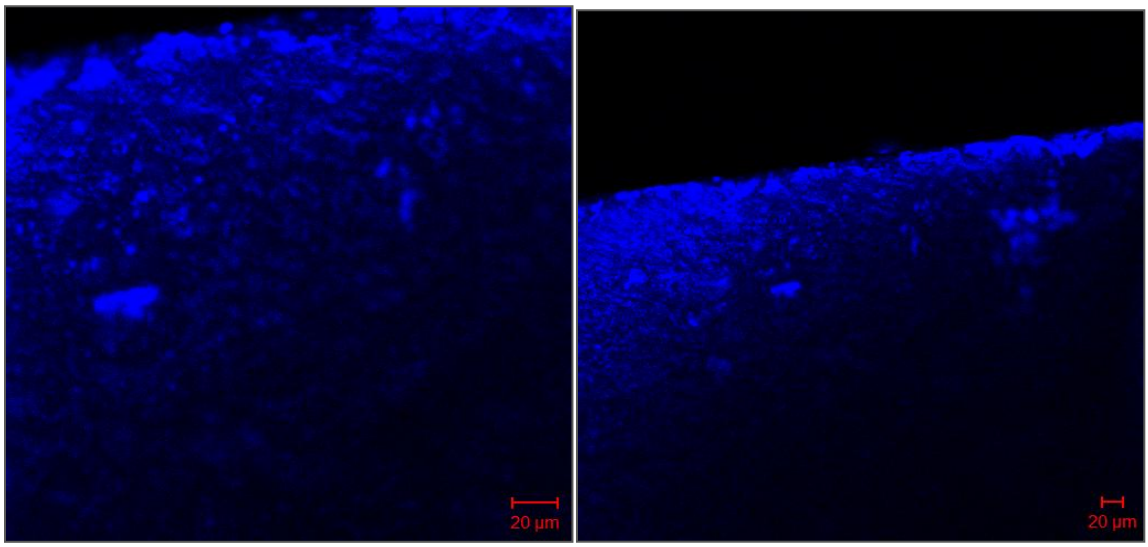

Fig. 3.7. a and b. Anode-associated biofilm on a piece of MEC electrode hybridized to EUB338 (blue) and embedded in a thin layer of agarose.

As can be seen in Fig. 3.7., the final optimized protocol allowed for visualization of cell structure at the single cell level.

3.5. Conclusions

Different protocols for MEC electrode embedding were tested in this part of the investigation. Initially, polyacrylamide, LR White, and agarose were examined to determine which would be best able to preserve the three dimensional structure of an anode-associated biofilm still attached to an electrode. The finalized protocol, embedding in 30 µl of 0.8% agarose, was found to be reliable, low cost, and, most importantly, was able to prevent biofilm destruction and provide clear images with distinct cellular structure. Now that an embedding protocol has been optimized and proven to be fully functional for the purpose of preserving biofilm structure on electrodes, it will important to take Z-stack images of biofilms, since all images previously obtained are single sections. It can be utilized further for performing FISH with more specific probes to investigate the colonization strategies of the microorganisms in these biofilms.

CHAPTER 4: CONCLUSIONS AND FUTURE WORK

Upon completing this study, it was discovered that an H-type MEC inoculated with activated sludge cultivates a community composed of mainly mainly *Delta/Epsilonproteobacteria, Firmicutes* and *Bacteroidetes.* It was also noted that this MEC community functions better with a stable community, where the biofilm community members remain in a steady state. Lastly,m it was discovered that, although the community was capable of reducing the overall abundance of methanogens, at day 110 methanogens still account for a significant amount of the community, indicating that methods of methane inhibition are necessary to pursue.

The continuation of this specific project has many facets that have yet to be investigated. In the short term there needs to be a more thorough FISH analysis of homogenized biofilm samples, using more specific probes in order to determine relative abundance of all relevant members of the community, such as *Pelobacter*, *Bacteroidetes* and *Epsilonproteobacteria*. This may lead to a clearer picture of how the community members can impact current density throughout a reactor's lifetime, since this study has already produced evidence that community changes correlate with current production. Furthermore, the embedding protocol outlined in Chapter 3, has yet to be utilized to its full potential. Z-stack images, (sets of images of planes at various depths within the sample) still need to be obtained in order to elucidate the three dimensional distribution of microorganisms within the anode-associated biofilm. This would reveal the spatial orientation of community on the electrode, possibly disclosing more information about anodal electron transfer.

It would be interesting to sample the electrode daily between day 0 and the end of batch mode, when current first stabilizes, using the FISH embedding protocol. This would allow for the determination of the early colonization strategy of the MEC community. It would be beneficial

to apply this both to samples from a regular ethanol-fed MEC (similar to the one in this study), as well as to samples from a setup where methanogenesis is inhibited, to determine if current can be stabilized and increased earlier on if methanogens are suppressed in the community. Lastly, it would be beneficial to run an MFC or MEC at Ryerson for the continuation and remainder of this project. Samples could be taken directly at the university, potentially improving results, since samples will not need to be stored on ice in transit for several days, allowing for immediate analysis of samples upon removal from the anode.

Overall, progress in improving the efficiency of MECs has progressed significantly in the last decade, with several groups focused on this research (Chapter 1). There are still many gaps in the literature but researchers are slowly closing them, especially as more microbiologists participate in MEC research and elucidate on the microbial community that participates in current generation.

CHAPTER 5: APPENDICES

Appendix A: FLUORESCENT *IN SITU* HYBRIDIZATION IMAGES

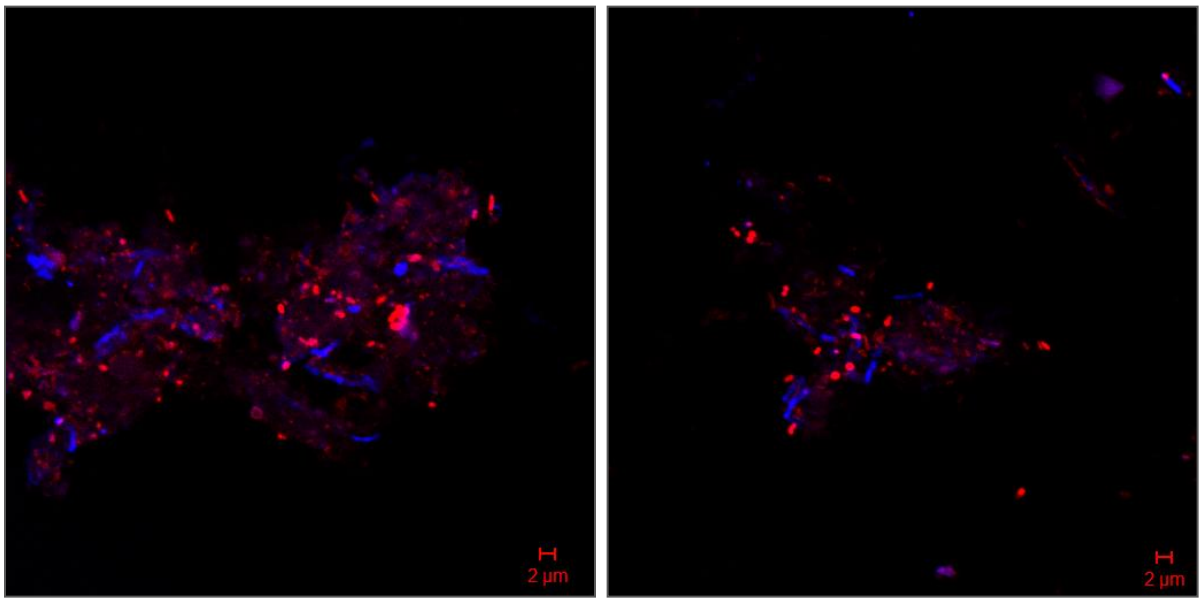

Fig. 6.1. a and b. FISH results using EUB 338 (blue) targeting most *Bacteria* and ARC915 (red) targeting *Archaea* applied to homogenized inoculum (day 0) samples from an ethanol-fed MEC inoculated with anaerobic digested sludge.

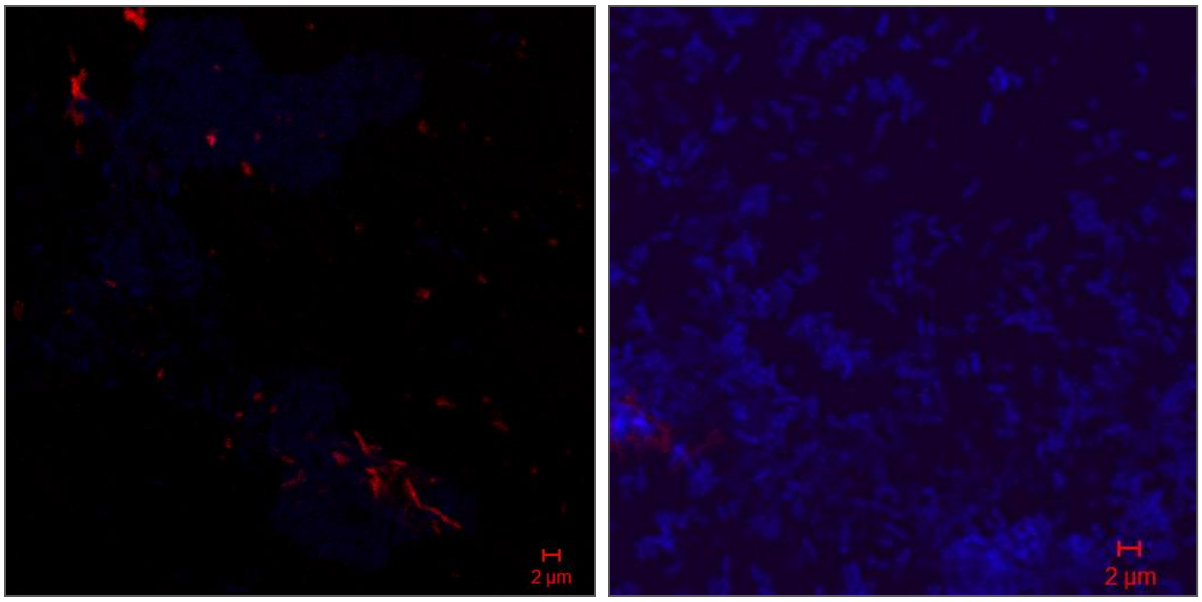

Fig. 6.2. a and b. FISH results using EUB 338 (blue) targeting most *Bacteria* and ARC915 (red) targeting *Archaea* applied to homogenized day 10 samples from an ethanol-fed MEC inoculated with anaerobic digested sludge.

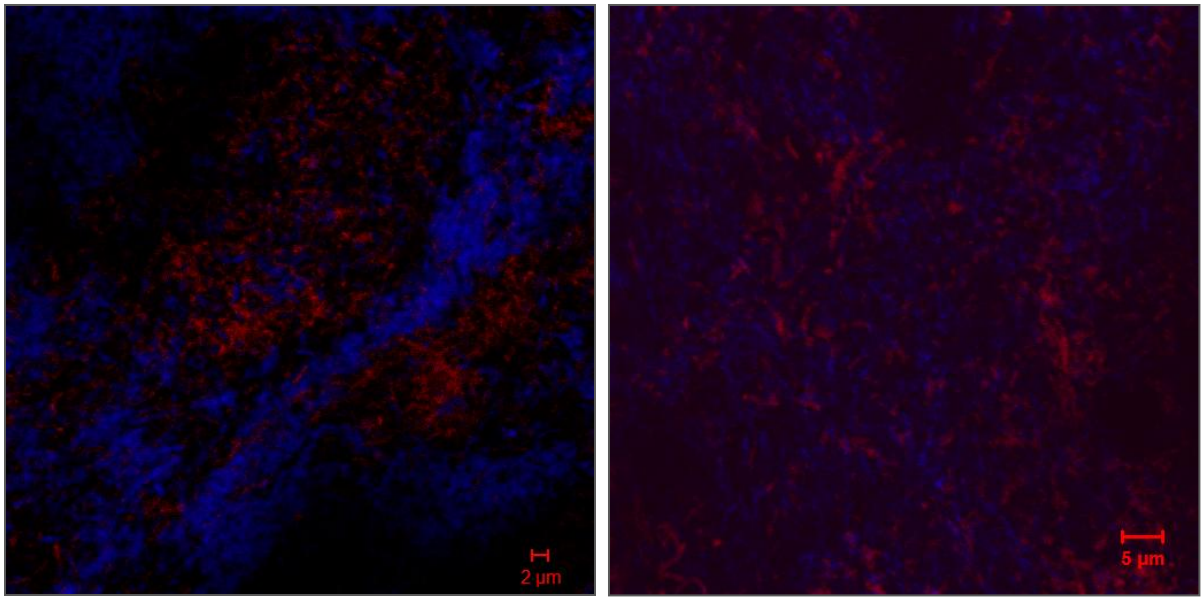

Fig. 6.3. a and b. FISH results using EUB 338 (blue) targeting most *Bacteria* and ARC915 (red) targeting *Archaea* applied to homogenized day 46 samples from an ethanol-fed MEC inoculated with anaerobic digested sludge.

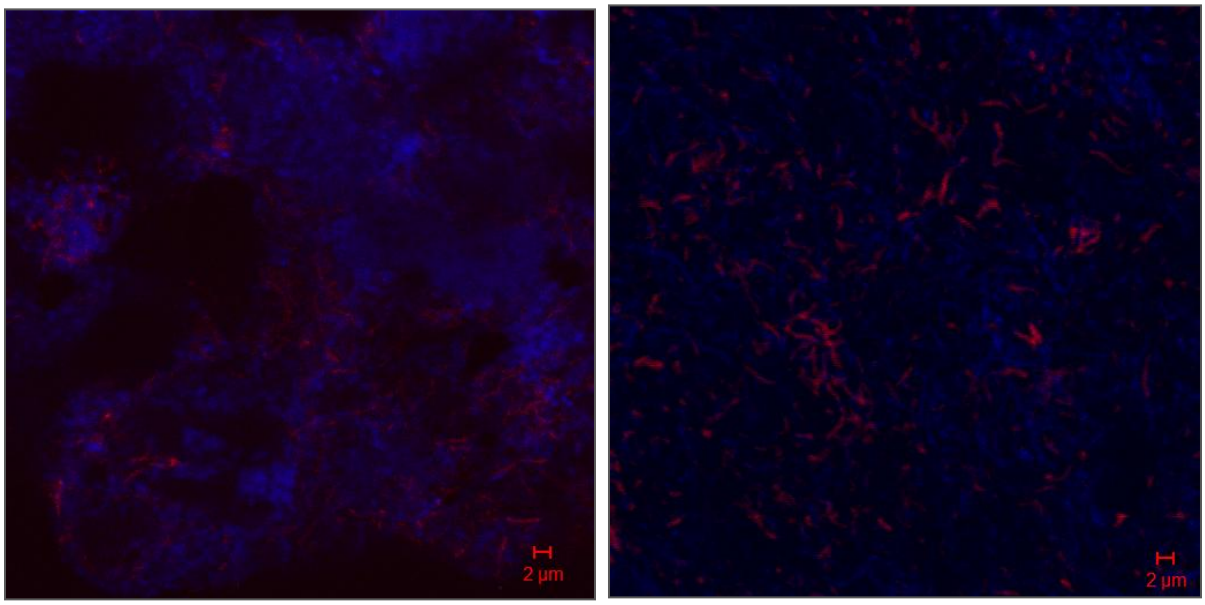

Fig. 6.4. a and b. FISH results using EUB 338 (blue) targeting most *Bacteria* and ARC915 (red) targeting *Archaea* applied to homogenized day 81 samples from an ethanol-fed MEC inoculated with anaerobic digested sludge.

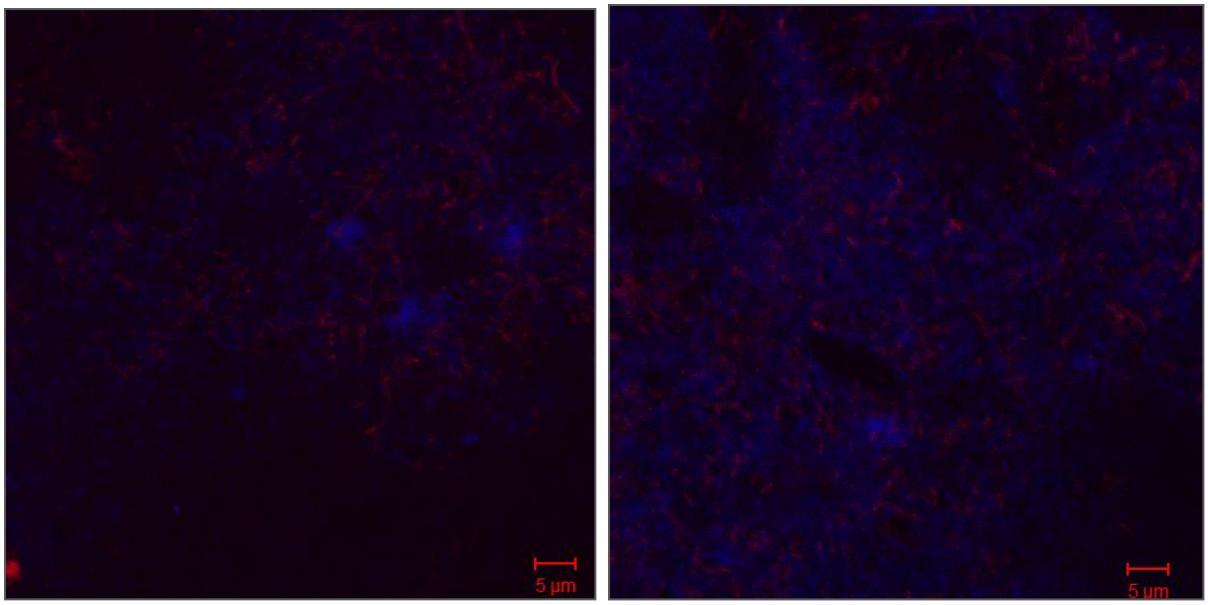

Fig. 6.5. a and b. FISH results using EUB 338 (blue) targeting most *Bacteria* and ARC915 (red) targeting *Archaea* applied to homogenized day 110 samples from an ethanol-fed MEC inoculated with anaerobic digested sludge.

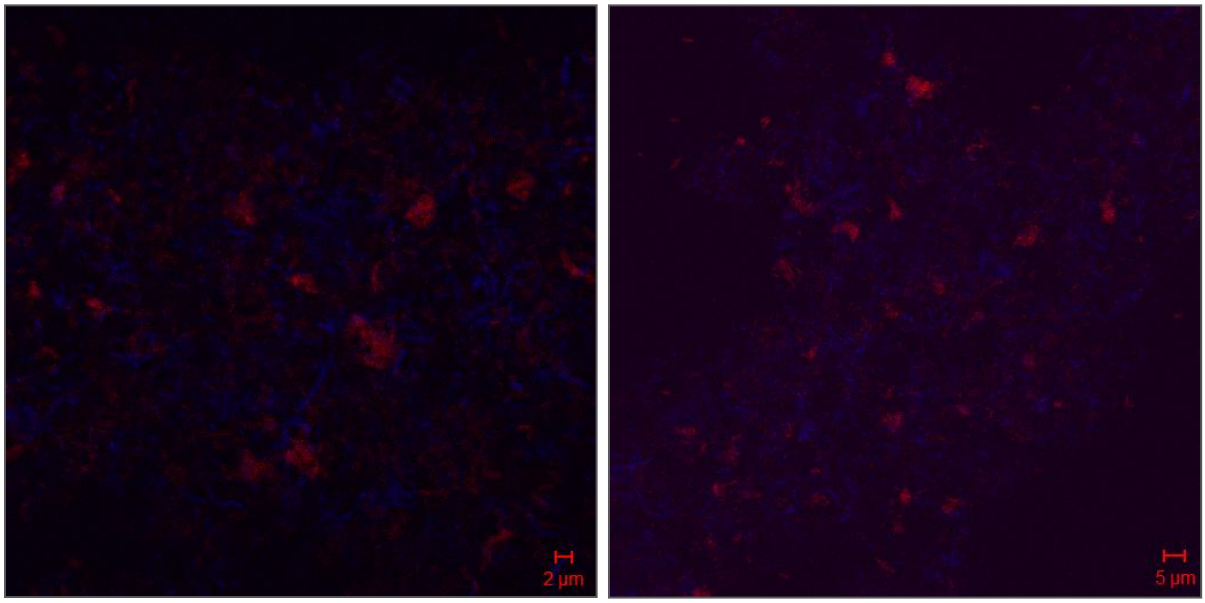

Fig. 6.6. a and b. FISH results using EUB 338 (blue) targeting most *Bacteria* and ARC915 (red) targeting *Archaea* applied to homogenized control electrode (day 110) samples from an ethanol-fed MEC inoculated with anaerobic digested sludge.

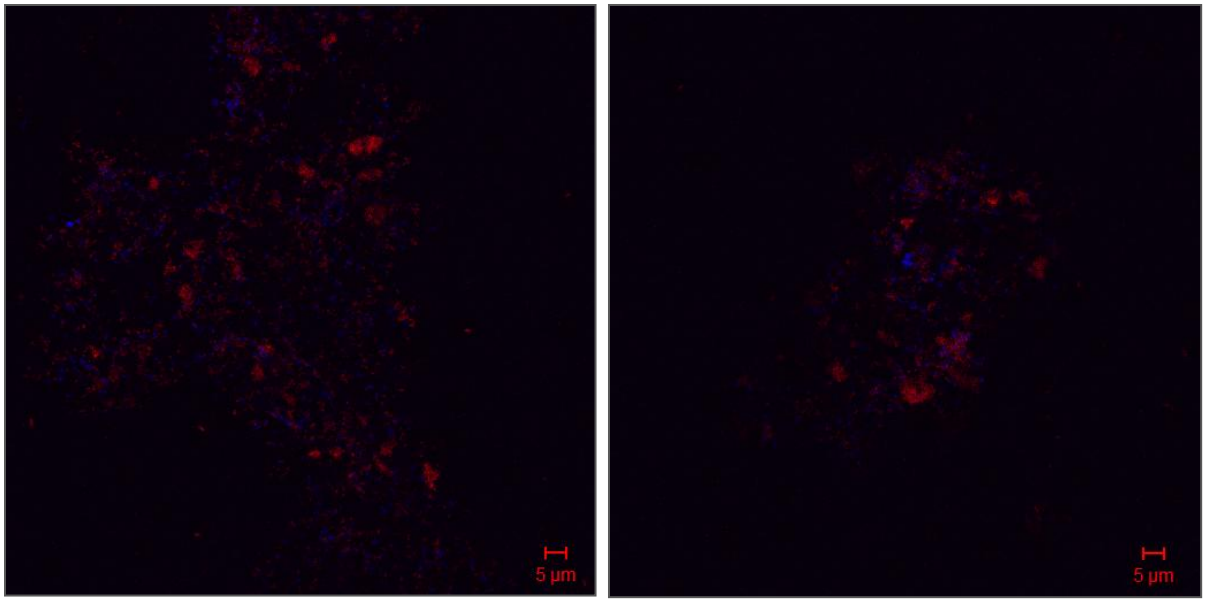

Fig. 6.7. a and b. FISH results using EUB 338 (blue) targeting most *Bacteria* and ARC915 (red) targeting *Archaea* applied to homogenized suspension (day 110) samples from an ethanol-fed MEC inoculated with anaerobic digested sludge.

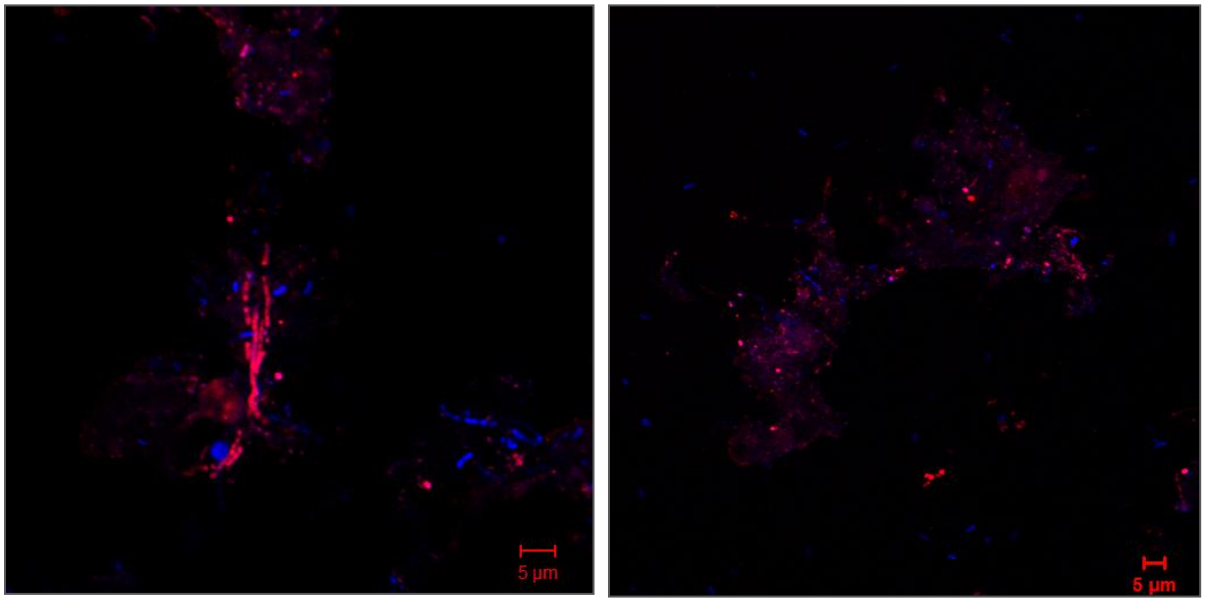

Fig. 6.8. a and b. FISH results using EUB 338 (blue) targeting most *Bacteria* and modSRB385 (red) targeting *Geobacter sp.* applied to Inoculum (day 0) samples from an ethanol-fed MEC inoculated with anaerobic digested sludge. Purple indicates the overlap of probe signals.

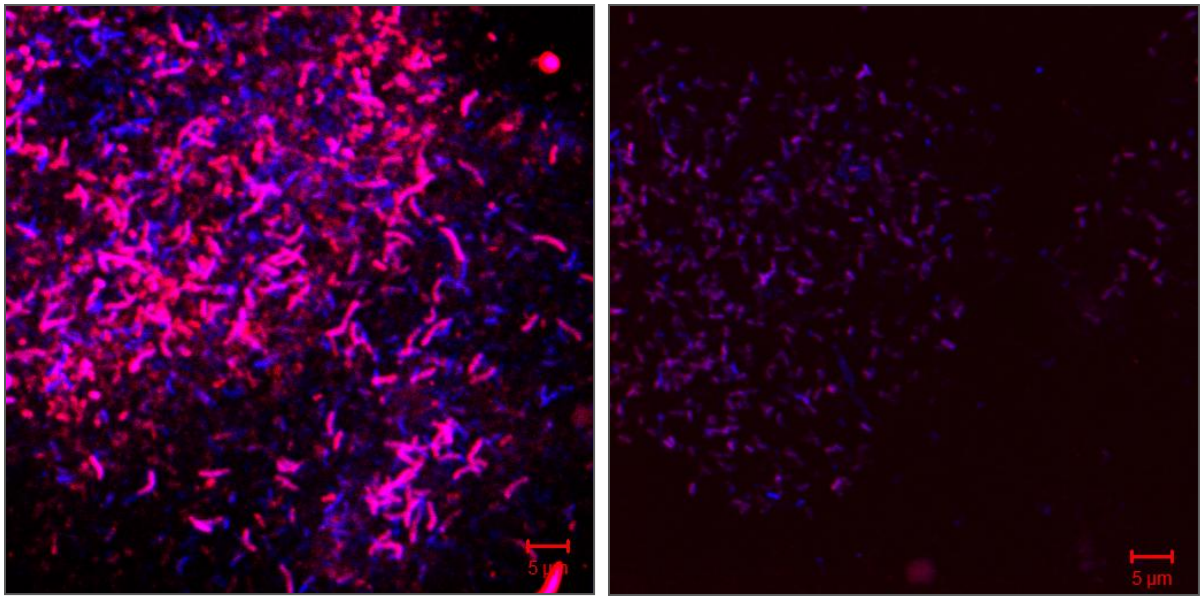

Fig. 6.9. a and b. FISH results using EUB 338 (blue) targeting most Bacteria and modSRB385 (red) targeting Geobacter sp. applied to day 46 samples from an ethanol-fed MEC inoculated with anaerobic digested sludge. Purple indicates the overlap of probe signals.

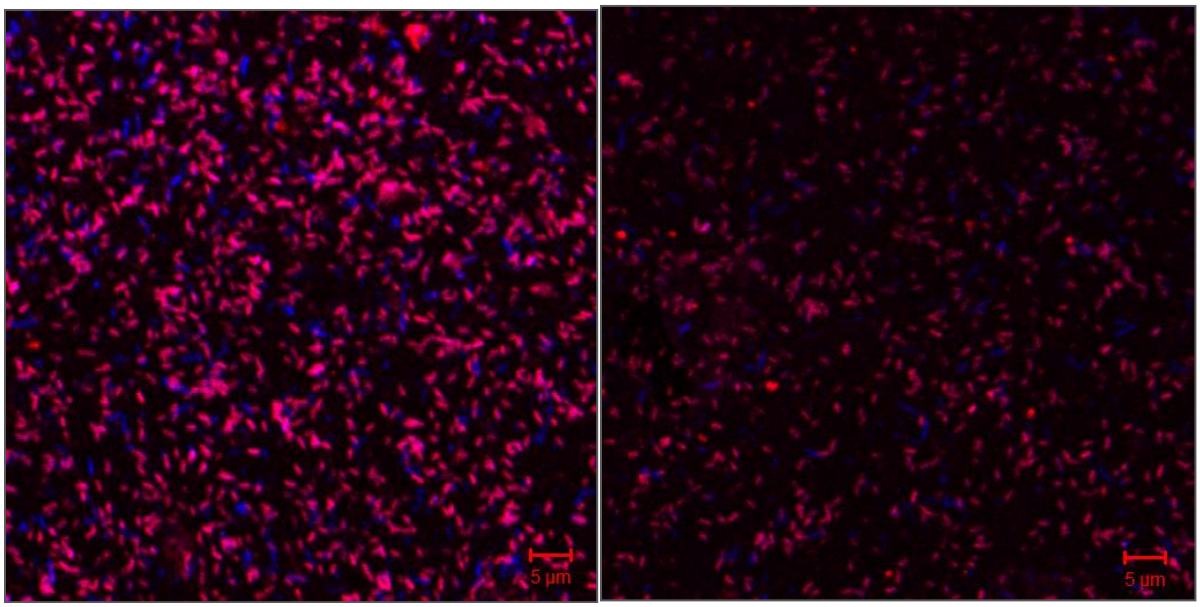

Fig. 6.10. a and b. FISH results using EUB 338 (blue) targeting most Bacteria and modSRB385 (red) targeting Geobacter sp. applied to day 81 samples from an ethanol-fed MEC inoculated with anaerobic digested sludge. Purple indicates the overlap of probe signals.

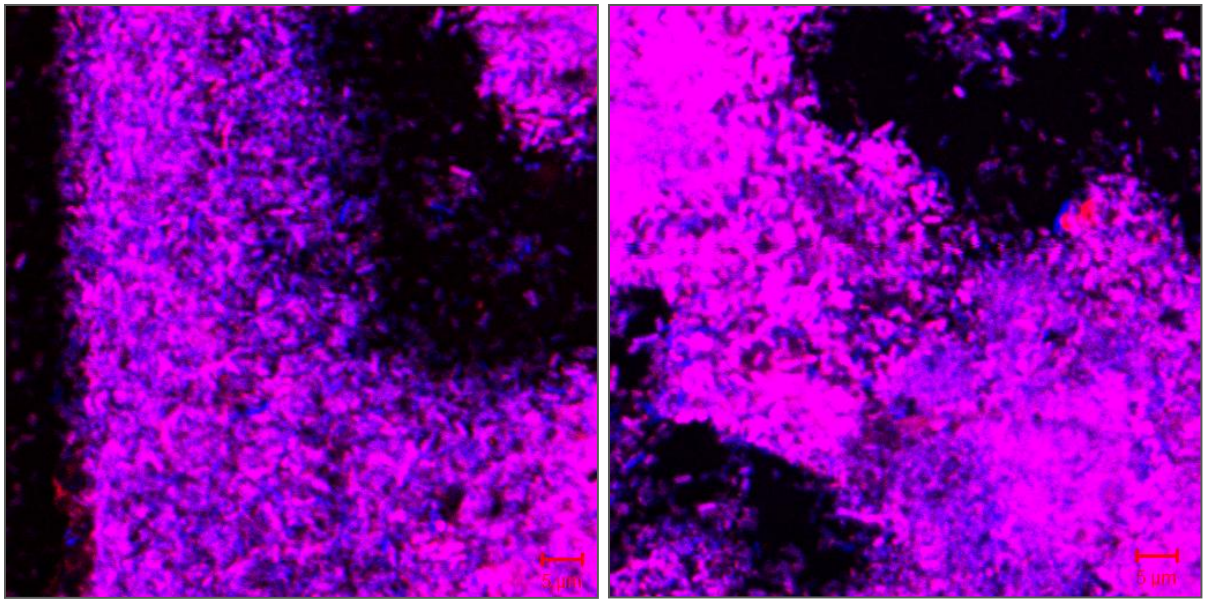

Fig. 6.11. a and b. FISH results using EUB 338 (blue) targeting most *Bacteria* and modSRB385 (red) targeting *Geobacter sp.* applied to day 110 samples from an ethanol-fed MEC inoculated with anaerobic digested sludge. Purple indicates the overlap of probe signals.

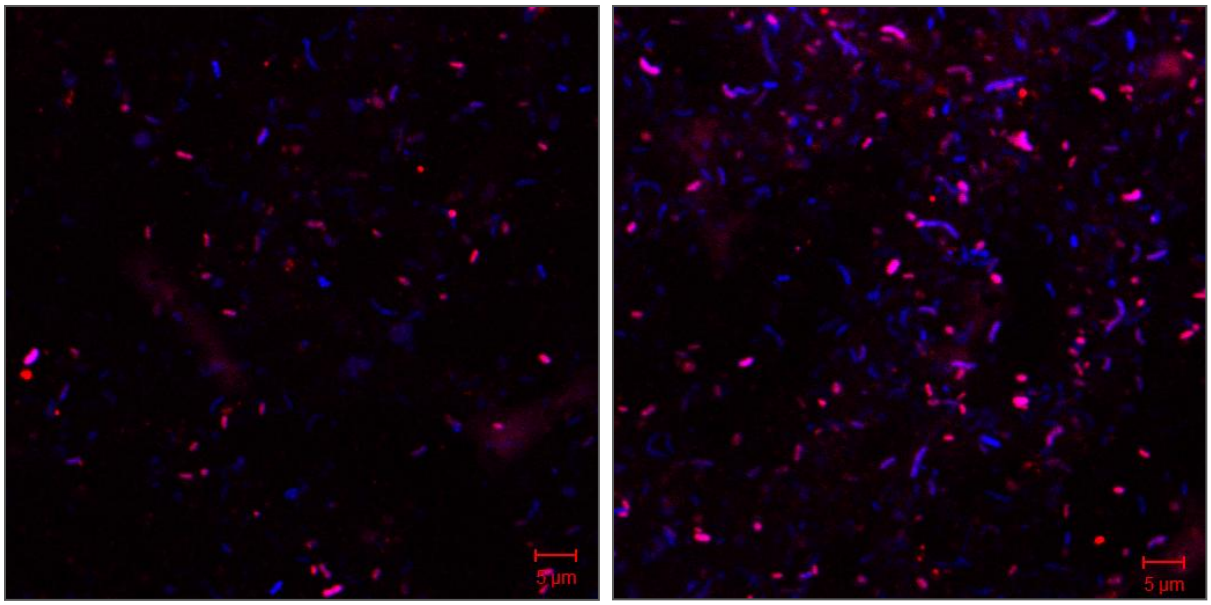

Fig. 6.12. a and b. FISH results using EUB 338 (blue) targeting most *Bacteria* and modSRB385 (red) targeting *Geobacter sp.* applied to negative control (day 110) samples from an ethanol-fed MEC inoculated with anaerobic digested sludge. Purple indicates the overlap of probe signals.

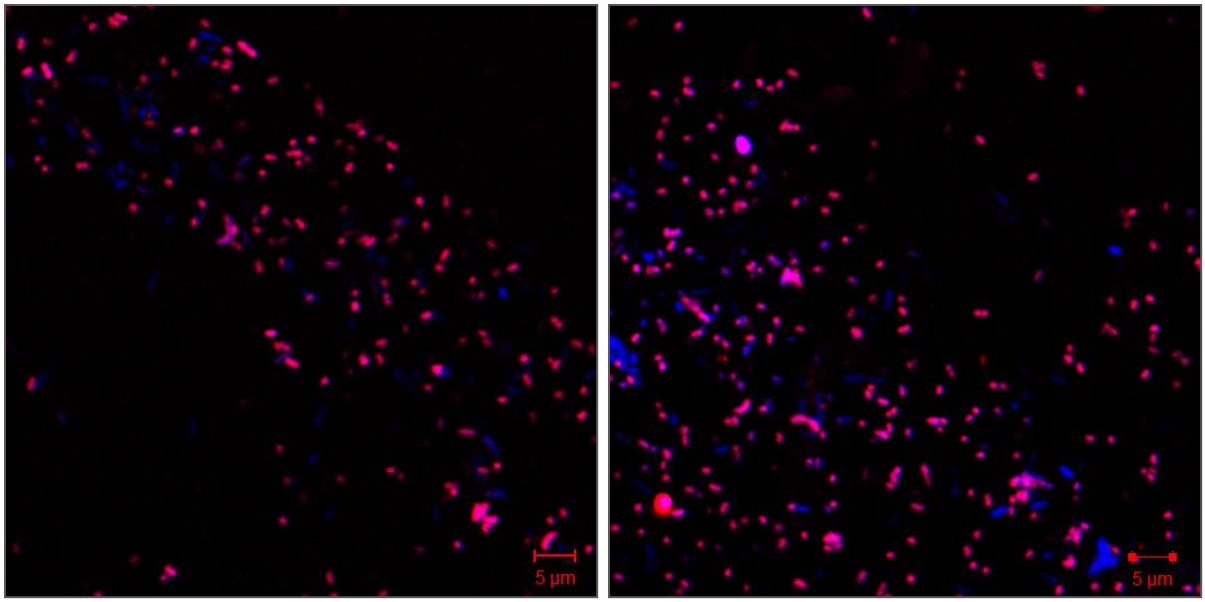

Fig. 6.13. a and b. FISH results using EUB 338 (blue) targeting most *Bacteria* and modSRB385 (red) targeting *Geobacter sp.* applied to suspension (day 110) samples from an ethanol-fed MEC inoculated with anaerobic digested sludge. Purple indicates the overlap of probe signals.

Appendix B: SUPPLEMENTARY DGGE IMAGES

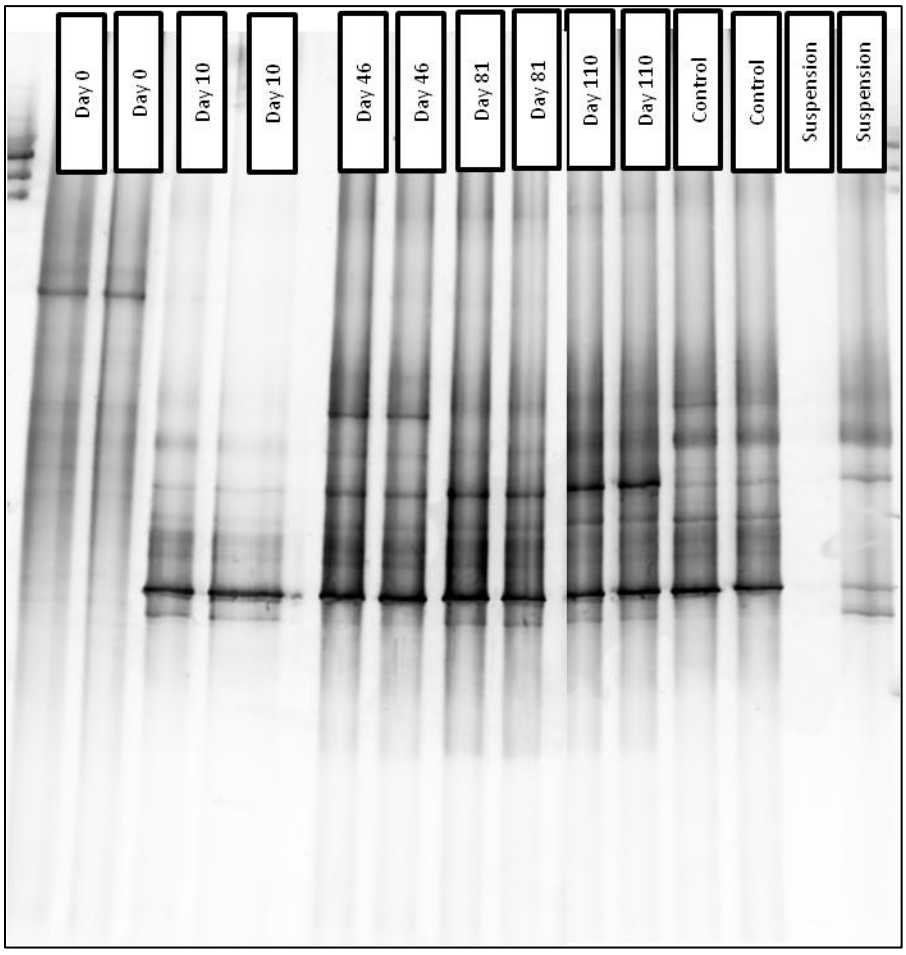

Fig. 6.14. DGGE gel of PCR products obtained with an bacterial primer set 1 (U341-GC and U758R) amplifying the 16S rRNA region in *Bacteria*. Samples were obtained from an ethanol fed H-type MEC inoculated with anaerobic digested sludge at days 0, 10, 46, 81, and 110 (including the suspension and a negative control electrode from day 110).

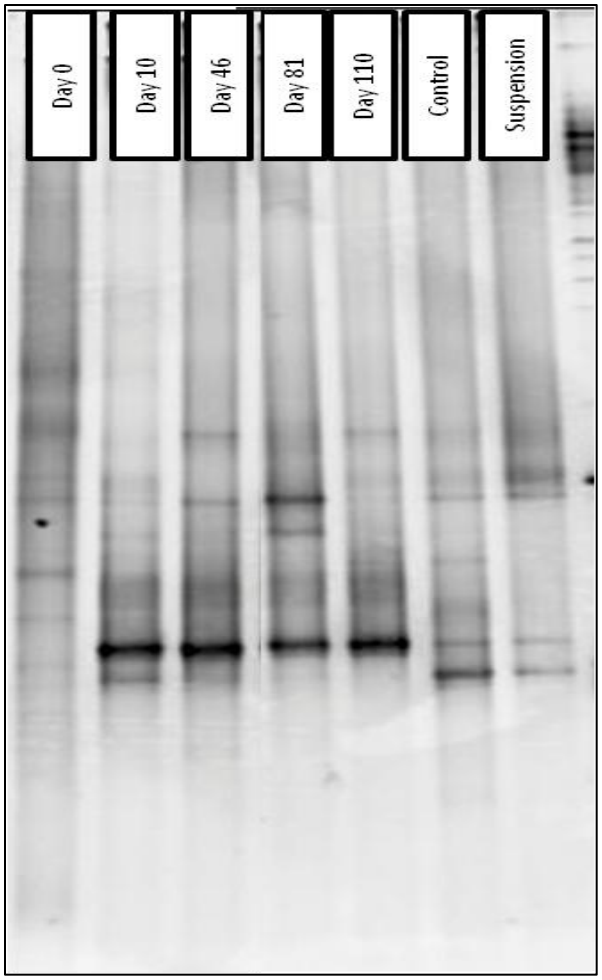

Fig. 6.15. DGGE gel of PCR products obtained with an bacterial primer set 2 (F1-GC and U519R) amplifying the 16S rRNA region in Bacteria. Samples were obtained from an ethanol fed H-type MEC inoculated with anaerobic digested sludge at days 0, 10, 46, 81, and 110 (including the suspension and a negative control electrode from day 110).

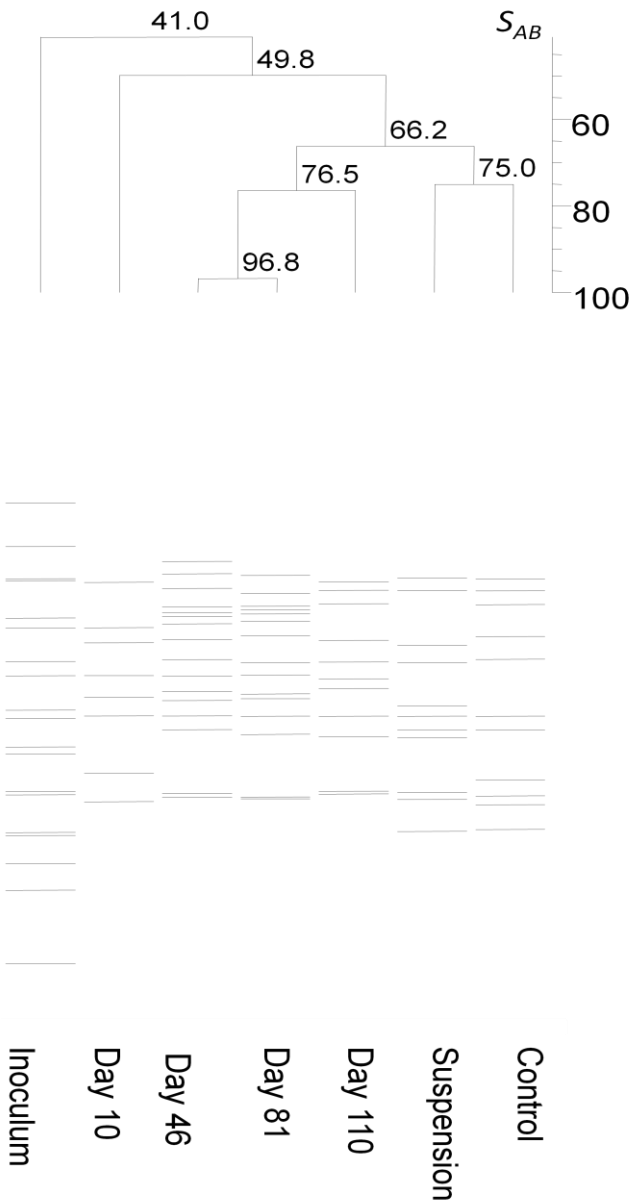

Fig. 6.16. Dendogram of PCR products obtained with bacterial primer set 2 (F1-GC and U519R) amplifying the 16S rRNA region in Bacteria. Samples were obtained from an ethanol fed H-type MEC inoculated with anaerobic digested sludge at days 0, 10, 46, 81, and 110 (including the suspension and a negative control electrode from day 110).

CHAPTER 6: REFERENCES

Aelterman, P., K. Rabaey, H. T. Pham, N. Boon, and W. Verstraete. 2006. Continuous Electricity Generation at High Voltages and Currents Using Stacked Microbial Fuel Cells Environmental Science and Technology. **40:**3388-3394.

Ahn, Y., and B. E. Logan. 2009. Effectiveness of domestic wastewater treatment using microbial fuel cells at ambient and mesophilic temperatures. Bioresources Technology. **101:**469-475.

Amann, R. I., B. J. Binder, R. J. Olson, S. W. Chisholm, R. Devereux, and D. A. Stahl. 1990. Combination of 16S rRNA-targeted oligonucleotide probes with flow cytometry for analyzing mixed microbial communitys. Applied Environmental Microbiology. **56:**1919-1925.

Amann, R. I., W. Ludwig, and K. H. Schleifer. 1995. Phylogenetic identification and *in situ* detection of individual microbial cells without cultivation. Microbiology and Molecular Biology Reviews. **59:**143-169.

Angenent, L. T., and B. A. Wrenn. 2008. Optimizing mixed-culture bioprocessing to convert wastes into bioenergy. ASM Press, Washington, DC, USA.

Bard, A. J., and L. R. Faulkner. 2000. Electrochemical Methods. Wiley & Sons, New York, USA.

Bass, H. W., W. F. Marshall, J. W. Sedat, D. A. Agard, and W. Z. Cande. 1997. Telomeres cluster de novo before the initiation of synapsis: a three-dimensional spatial analysis of telomere positions before and during meiotic prophase. Journal of Cell Biology. **137:**5-18.

Bowling, A.J., and K. C. Vaughn. 2008. A simple technique to minimize heat damage to specimens during thermal polymerization of LR White in plastic and gelatin capsules. Journal of Microscopy. **231:**186-189.

Burggraf, S., T. Mayer, R. Amann, S. Schadhauser, C. R. Woese, and K. O. Stetter. 1994. Identifying members of the domain Archaea with rRNA-targeted oligonucleotide probes. Applied and Environmental Microbiology. **60:**3112-3119.

Call, D., and B. E. Logan. 2008. Hydrogen production in a single chamber microbial electrolysis cell (MEC) lacking a membrane. Environmental Science and Technology. **42:**3401-3406.

Call, D., M. D. Merrill, and B. E. Logan. 2008. High surface area stainless steel brushes as cathodes in microbial electrolysis cells. Environmental Science and Technology. **43:**2179-2183.

Chae, K. J., M. J. Choi, J. Lee, F.F. Ajayi, and I. S. Kim. 2008. Biohydrogen production via biocatalyzed electrolysis in acetate-fed bioelectrochemical cells and microbial community analysis. International Journal of Hydrogen Energy. **33:**5184-5192.

Chae, K. J., M. J. Choi, K. Y. Kim, F.F. Ajayi, I. S. Chang, and I. S. Kim. 2010. Selective inhibition of methanogens for the improvement of biohydrogen production in microbial electrolysis cells. International Journal of Hydrogen Energy. **35:**13379-13386

Chen, X., D. B. Cho, and P. C. Yang. 2010. Double staining immunohistochemistry. North American Journal of Medical Science. **2:**241-245.

Cheng, S., and B.E. Logan. 2007. Ammonia treatment of carbon cloth anodes to enhance power generation of microbial fuel cells. Electrochemistry Communications. **9:**492-496.

Cheng, S., and B. E. Logan. 2007. Sustainable and efficient biohydrogen production via electrohydrogenesis. Proceedings of the National Academy of Sciences of the United States of America. **104:**18871-18873.

Cheng, S., and B. E. Logan. 2011. High hydrogen production rate of microbial electrolysis cell (MEC) with reduced electrode spacing. Bioresource Technology. **102:**3571-357.

Cheng, S., H. Liu, and B.E. Logan. 2006. Increased performance of single chamber microbial fuel cells using an improved cathode structure. Electrochemistry Communications. **8:**489-494.

Chaudhuri, S. K., and D. R. Lovley. 2003. Electricity generation by direct oxidation of glucose in mediatorless microbial fuel cells. Nature Biotechnology Letters. **21:**1229-1232.

Christensen, B. B., C. Sternberg, J. B. Andersen, R. J. Palmer Jr., A. T. Nielsen, M. Givskov, and S. Molin. 1999. Molecular tools for study of biofilm physiology**. 310:**20-42.

Chung, K., and Okabe, S. 2009. Continuous power generation and microbial community structure of the anode biofilms in a three-stage microbial fuel cell system. Applied Microbiology and Biotechnology. **83:**965-977.

Clauwaert, P., D. Vanderha, N. Boon, K. Verbeken, M. Varhaege, K. Rabaey, and W. Verstraete. 2007. Open air biocathode enables effective electricity generation with microbial fuel cells. Environmental Science and Technology. **41:**7564-7569.

Cusick, R. D., P. D. Kiely, and B. E. Logan. 2010. A monetary comparison of energy recovered from microbial fuel cells and microbial electrolysis cells fed winery or domestic wastewaters. International Journal of Hydrogen Energy. **35:**8855-8861.

Debabov, V. G. 2008. Electricity from microorganisms. Microbiology. **77:**123-131.

Du, Z., H. Li, and T. Gu. 2007. A state of the art review on microbial fuel cells: A promising technology for wastewater treatment and bioenergy. Biotechnology Advances. **25:**474-482.

Eickhorst, T., and R. Tippkotter. 2008. Improved detection of soil microorganisms using fluorescence *in situ* hybridization (FISH) and catalyzed reporter deposition (CARD-FISH). Soil Biology and Biochemistry. **40:**1883-1891.

Freguia, S., K. Rabaey, Z. Yuan, and J. Keller. 2007. Non-catalyzed cathodic oxygen reduction at graphite granules in microbial fuel cells. Electrochimica Acta. **53:**598-603.

Friedrich, A. B., H. Merkert, T. Fendert, J. Hacker, P. Proksch and U. Hentschel. 1999. Microbial diversity in the marine sponge *Aplysina cavernicola* (formerly *Verongia cavernicola*) analyzed by fluorescence *in situ* hybridization (FISH). Marine Biology. 134:461-470.

Fung, C.Y., J. Lee, I. S. Chang, and B. H. Kim. 2006. Bacterial communities in microbial fuel cells enriched with high concentrations of glucose and glutamate. Journal of Microbiology and Biotechnology. **16:**1481-1484.

Germroth, P. G., R. G. Gourdie, and R. P. Thomson. 1995. Confocal microscopy of thick sections from acrylamide gel embedded embryos. Microscopy research and technique. **30:**513-520.

Gorby, Y. A., S. Yanina, J. S. McLean, K. M. Rosso, D. Moyles, A. Dohnalkova, T. J. Beveridge, I. C. Chang, B. H. Kim, K. S. Kim, D. E. Culley, S. E. Reed, M. F. Romine, D. E. Saffarini, E. A. Hill, L. Shi, D. A. Elias, D. W. Kennedy, G. Pinchuk, K. Watanabe, S. I. Ishii, B. Logan, K. H. Nealson, and J. K. Fredrickson. 2006. Electrically conductive bacterial nanowires produced by *Shewanella oneidensis* strain MR-1 and other microorganisms. Proceedings of the National Academy of Sciences of the United States of America. **103:**11358-11363.

Gregory, K. B., D. R. Bond, and D. R. Lovley. 2004. Graphite electrodes as electron donors for anaerobic respiration. Environmental Microbiology. **6:**596-604.

Gros, O, and L. C. Maurin. 2008. Easy flat embedding of oriented samples in hydrophilic resin (LR White) under controlled atmosphere: Application allowing both nucleic acid hybridizations (CARD-FISH) and ultrastructural observations. Acta histochemica. **110:**427-431.

Gupta, G., B. Sikarwar, V. Vasudevan, M. Boopathi, O. Kumar, B. Singh, and R. Vijayaraghavan. 2011. Microbial fuel cell technology: a review on electricity generation. Journal of Cell and Tissue Research. **11:** 2631-2654.

Hausen, P., and C. Dreyer. 1981. The use of polyacrylamide as an embedding medium for immunohistochemical studies of embryonic tissues. Biotechnic and Histochemistry. **56:**287-293.

Hofstad, T., I. Olsen, E. R. Eribe, E. Falsen, M. D. Collins, and P. A. Lawson. 2000. Dysgonomonas gen. nov. to accommodate Dysgonomonas gadei sp. nov., an organism isolated from a human gall bladder, and Dysgonomonas capnocytophagoides (formerly CDC group DF-3). International Journal of Systematic and Evolutionary Microbiology. **50:**2189-2195.

Holladay, J. D., J. Hua, D. L. Kinga, and Y. Wang. 2009. An overview of hydrogen production technologies. Catalysis Today. **139:**244-260.

Hu, H., Y. Fana, and H. Liu. 2008. Hydrogen production using single-chamber membrane-free microbial electrolysis cells. Water research. **42:**4172-4178.

Istok, J. D., M. Park, M. Michaelsen, A. M. Spain, L. R. Krumholz, C. Liu, J. McKinley, P. Long, E. Rodon, A. D. Peacock, and B. Baldwin. 2010. A thermodynamically-based model for predicting microbial growth and community composition coupled to system geochemistry: application to uranium bioreduction. Journal of Contaminant Hydrology. **112:**1-14.

Jeremiasse, A. W., H. Hamelers, M. Saakesa, and C. J. N. Buisman. 2010. Ni foam cathode enables high volumetric H_2 production in a microbial electrolysis cell. International Journal of Hydrogen Energy. **35:**12716-12723.

Jiang, W., J. Chang, J. Jakana, P. Weigele, J. King, and W. Chiu. 2006. Structure of epsilon15 bacteriophage reveals genome organization and DNA packaging/injection Apparatus. Nature Letters. **439:**612-616.

Jung, S., and J. M. Regan. 2007. Comparison of anode bacterial communities and performance in microbial fuel cells with different electron donors. Applied Microbial and Cell Physiology. **77:**393-402.

Kadoshin, S., T. Nishiyama, and T. Ito. 2000. The trend in current and near future energy consumption from a statistical perspective. Applied Energy. **67:**407-417.

Kiely, P. D., R. Cusick, D. F. Call, P. A. Selembo, J. M. Regan, and B.E. Logan. 2011. Anode microbial communities produced by changing from microbial fuel cell to microbial electrolysis cell operation using two different wastewaters. Bioresource Technology. **102:**388-394.

Kim, H. J., M. S. Hyun, I. S. Chang, and B. H. Kim. 1999. A microbial fuel cell type lactate biosensor using a metal reducing biosensor, *Shewanella putrafaciens.* Microbiology and Biotechnology. **9:**365-367.

Kim, J. R., S. Cheng, S. E. Oh, and B. E. Logan. 2007. Power generation using different cation, Anion, and Ultrafiltration membranes in microbial fuel cells. Environmental Science and Technology. **41:**1004-1009.

Kim, J. R., S. K. Jung, J. M. Regan, and B. E. Logan. 2006. Electricity generation and microbial community analysis of alcohol powered microbial fuel cells. Bioresource Technology. **98:**2568-2577.

Lalaurette, E., S. Thammannagowda, A. Mohagheghi, P. C. Maness, and B. E. Logan. 2009. Hydrogen production from cellulose in a two-stage process combining fermentation and electrohydrogenesis. International Journal of Hydrogen Energy. **34:**6201-6210.

Lee, H. S., P. Parameswaran, A. Kato-Marcus, C. I. Torres, and B. E. Rittman. 2008. Evaluation of energy-conversion efficiencies in microbial fuel cells (MFCs) utilizing fermentable and non-fermentable substrates. Water Research. **42:**1501-1510.

Lee, H. S., C. I. Torres, P. Parameswaran, and B. E. Rittman. 2009. Fate of H_2 in an upflow single-chamber microbial electrolysis cell using a metal-catalyst-free cathode. Environmental Science and Technology. **43:**7971-7976.

Lee, H. S., W. F. J. Vermaas, and B. E. Logan. 2010. Biological hydrogen production: prospects and challenges. Trends in Biotechnology. **28:**262-271.

Leitch, A. R., W. Mosgoller, T. Schwarzacher, M. D. Bennett, and J. S. Heslop-Harrison. 1990. Genomic *in situ* hybridization to sectioned nuclei shows chromosome domains in grass hybrids. Journal of Cell Science. **95:**335-341.

Lies, D. P., M. E. Hernandez, A. Kappler, R. E. Mielke, J. A. Gralnick, and D. K. Newman. 2005. *Shewanella oneidensis* MR-1 uses overlapping pathways for iron reduction at a distance and by direct contact under conditions relevant for biofilms. Applied and Environmental Microbiology. **71:**4414-4426.

Liu, H., S. Grot, and B. E. Logan. 2005. Electrochemically assisted microbial production of hydrogen from acetate. Environmental Science and Technology. **39:**4317-4320.

Liu, H., H. Hu, J. Chignell, and Y. Fan. 2010. Microbial electrolysis: novel technology for hydrogen production from biomass. Biofuels. **1:**129-142.

Logan, B. E. 2008. Microbial Fuel Cells. John Wiley and Sons Inc., New Jersey, USA.

Logan, B. E., and J. M. Regan. 2006. Electricity-producing bacterial communities in microbial fuel cells. Trends in Microbiology. **14:**512-518.

Logan, B. E., B. Hamelers, R. Rozendal, U. Schroder, J. Keller, S. Freguia, P. Aelterman, W. Verstraete, and K. Rabaey. 2006. Microbial Fuel Cells: Methodology and Terminology. Environmental Science and Technology. **40:**5181-5192.

Logan, B. E. 2009. Exoelectrogenic bacteria that power microbial fuel cells. Nature Reviews Microbiology. **7:**375-381.

Logan, B. E. 1998. A review of chlorate and perchlorate reducing microorganisms. Bioremediation: **2:**69-79.

Lovley, D. R. 2006. Bug juice: harvesting electricity with microorganisms. Nature Reviews, Microbiology. **4:**497-508.

Lovley, D. R. 2006. Microbial fuel cells: novel microbial physiologies and engineering approaches. Current Opinion in Biotechnology. **17:**327-332.

Lovley, D. R. 2008. The Microbe Electric: conversion of organic matter to electricity. Current Opinion in Biotechnology. **19:**564-571.

Lower, S. K., M.F. Hochella, and T. J. Beveridge. 2001. Bacterial recognition of mineral surfaces: nanoscale interactions between *Shewanella* and α-FeOOH. Science. **292:**1360-1363.

Manz, W., R. Amann, W. Ludwig, M. Wagner, and K. H. Schleifer. 1992. Phylogenetic oligodeoxynucleotide probes for the major subclasses of Proteobacteria: Problems and solutions. System. Appl. Microbiol. **15:**593-600.

Mehanna, M., P. D. Kiely, D. F. Call, and B. E. Logan. 2010. Microbial electrodialysis cell for simultaneous water desalination and hydrogen gas production. Environmental Science and Technology. **44:**9578-9583.

Møller, S., C. Sternberg, J. B. Andersen, B. B. Christensen,J. L. Ramos, M. Givskov, and S. Molin. 1997. *In situ* gene expression in mixed-culture biofilms: evidence of metabolic interactions between community members. Applied and Environmental Microbiology. **64:**721-732.

Muyzer, G., E. C. De Waal, and A. G. Uitterlinden. 1993. Profiling of complex microbial communitys by denaturing gradient gel electrophoresis analysis of polymerase chain reaction-amplified gene coding for 16S rRNA. Appl. Environmental Microbiology. **59:**695-700 .

Myers, C. M., and J. M. Myers. 2004. The outer membrane of cytochromes of *Shewanella oneidensis* MR-1 are lipoproteins. Letter in Applied Microbiology. **39:**466-470.

Nevin, K. P., and D. R. Lovley. 2002. Mechanisms for Iron(III) Oxide Reduction in Sedimentary Environments. Geomicrobiology Journal. **19**:141-159.

Newman, G.R., B. Jasani, and E.D. Williams. 1982. The preservation of ultrastructure and antigenicity. Journal of Microscopy. **127:**RP5-RP6.

Nielsen , M. E., D. M. Wu, P. R. Girguis, and C. E. Reimers. 2009. Influence of substrate on electron transfer mechanisms in chambered benthic microbial fuel cells. Environmental Science and Technology. **43:**8671–8677.

Nussbaumer, A. D., C. R. Fisher, and M. Bright. 2006. Horizontal endosymbiont transmission in hydrothermal vent tubeworms. Nature. **441:**345-348.

Parameswaran, P., C. I. Torres, H. S. Lee, R. Krajmalnik-Brown, and B. Rittmann. 2009. Syntrophic Interactions Among Anode Respiring Bacteria (ARB) and Non-ARB in a Biofilm Anode: Electron Balances. Biotechnology and Bioengineering. **103:**513-523.

Parameswaran, P., C. I. Torres, H. S. Lee, B. E. Rittmann, and R. Krajmalnik-Brown. 2011. Hydrogen consumption in microbial electrochemical systems (MXCs): the role of homo-acetogenic bacteria. Bioresource Technology. **102:** 263–271.

Parameswaran, P., H. Zhang, C. I. Torres, B.E. Rittmann, and R. Krajmalnik-Brown. 2010. Microbial community structure in a biofilm anode fed with a fermentable substrate: The significance of hydrogen scavengers. Biotechnology and Bioengineering. **105:**69-78.

Parameswaran, P., unpublished data, personal communication.

Penner, J. L. 1988. The genus *Campylobacter*: A decade of progress. Clinical Microbiology Reviews. **1:**157-172.

Pernthaler, J., F. O. Glöckner, W. Schönhuber, and R. I. Amann. 2001. Fluorescence *in situ* hybridization, p. 207-226. *In* J. Paul (ed.), Methods in Microbiology: Marine Microbiology, In J. Paul ed., Academic Press Ltd, London, London, England.

Pernthaler, A., J. Pernthaler, and R.I. Amann. 2002. Fluorescence *in situ* hybridization and catalyzed reporter deposition for the identification of marine bacteria. Applied Environmental Microbiology. **68:**3094-3101.

Potter, M. C. 1912. Electrical effects accompanying the decomposition of organic compounds. Proceedings of the Royal Society B, Biological Sciences. **84:**260-76.

Rabaey, K., N. Boon, S. D. Siciliano, M. Verhaege, and W. Verstaete. 2004. Biofuel cells select for microbial consortia that self mediate electron transfer. Applied and Environmental Microbiology. **9:**5373-5382.

Rabaey, K., G. Lissens, S. D. Siciliano, and W. Verstraete. 2003. A microbial fuel cell capable of converting glucose to electricity at high rate and efficiency. Biotechnology Letters. **25:**1531-1535.

Rabaey, K., K. Van de Sompel, L. Maignien, N. Boon, P. Aelterman, P. Clauwaert, L. De Schamphelaire, H. T. Pham, J. Vermeulen, J. Verhaege, P. Lens, and W. Verstraete. 2006. Microbial fuel cells for sulfide removal. Environmental Science and Technology. **40:**5218-5224.

Rabaey, K., and W. Verstraete. 2005. Microbial fuel cells: novel biotechnology for energy generation. Trends in Biotechnology. **23:**291-298.

Reguera, G., K. D. McCarthy, T. Mehta, J. S. Nicoll, M. T. Tuominen, and D. B. Lovley. 2005. Extracellular electron transfer via microbial nanowires. Natures Letters. **435:**1098-1101.

Reimer, C. E., L. M. Tender, S. Fertig, and W. Wang. 2001. Harvesting energy from the marine sediment-water interface. Environmental Science and Technology. **35:**192-195.

Ren, Z, T. E. Ward, and J. M. Regan. 2007. Electricity production from cellulose in a microbial fuel cell using a defined binary culture. Environmental Science and Technology. **41:**4681-4686.

Ren, Z, M. Steinberg, and J. M. Regan. 2008. Electricity production and microbial biofilm characterization in cellulose-fed microbial fuel cells. Water Science and Technology. **58:**617-622.

Rezaei, F., D., Xing, R. Wagner, J. M. Regan, T. L. Richard, and B. E. Logan. 2009. Simultaneous cellulose degradation and electricity production by enterobacter cloacae in a microbial fuel cell. Applied and Environmental Microbiology. **75:**3673-3678.

Richter, H, M. Lanthier, K.P. Nevin, D.R. Lovley. 2007. Lack of electricity production by *Pelobacter carbinolicus* indicates that the capacity for Fe(III) oxide reduction does not necessarily confer electron transfer ability to fuel cell anodes. Applied Environmental Microbiology. **73:**5346-5353.

Rittmann, B.E. 2008. Opportunities for renewable bioenergy using microorganisms. Biotechnology and Bioengineering. **100:**203-212.

Rodrigo, M. A., P. Canizares, J. Lobato, R. Paz, C. Saez, and J.J. Linares. Production of electricity from the treatment of urban waste water using a microbial fuel cell. Journal of Power Sources. **169:**198-204

Rolleke, S., G. Muyzer, C. Wawer, G. Wanner, and W. Lubitz. 1996. Identification of bacteria in a biodegraded wall painting by denaturing gradient gel electrophoresis of PCR-amplified gene fragments coding for 16S rRNA. Applied and Environmental Microbiology. **62:**2059-2065.

Rozendal, R. A., A. W. Jeremiasse, H. V. M. Hamelers, C. J. N. Buisman. 2008. Hydrogen production with a microbial biocathode. Environmental Science and Technology. **42:**629-634.

Rozendal, R. A., H. V. M. Hamelers, and C. J. N. Buisman. 2006. Effects of membrane cation transport on pH and microbial fuel cell performance. Environmental Science and Technology. **40:** 5206-5211.

Sato N, K. Sakamaki , N. Terada, K. Arai, and A. Miyajima. 1993. Signal transduction by the high-affinity GM-CSF receptor: two distinct cytoplasmic regions of the common beta subunit responsible for different signalling. EMBO Journal. **12:**4181-4189.

Schink, B. 1983. Fermentation of 2,3-butanediol by Pelobacter carbinolicus sp. nov., and Pelobacter propionicus sp. nov., and evidence for propionate formation from C2 compounds. Archives of Microbiology. **137:**33-41.

Selembo, P.A., M. D. Merrill, B. E. Logan. 2009. The use of stainless steel and nickel alloys as low-cost cathodes in microbial electrolysis cells. Journal of Power Sources. **190:**271-278.

Show, K-Y., D-J. Leeb, and J-S. Chang. 2011. Bioreactor and process design for biohydrogen production. Bioresource Technology. *In press.*

Stahl, D.A., and R. Amann. 1991. Nucleic Acid Techniques in Bacterial Systematics. John Wiley and Sons Ltd., Chichester, UK.

Torres, C. I., A. K. Marcus, and B. E. Rittmann. 2007. Kinetics of consumption of fermentation products by anode-respiring bacteria. Applied Microbiology and Biotechnology. **77:**689-697.

Torres, C.I., A. K. Marcus, H. S. Lee, P. Parameswaran, R. Krajmalnik-Brown, and B. E. Rittmann. 2010. A kinetic perspective on extracellular electron transfer by anode-respiring bacteria. FEMS Microbiology Review. **34:**3-17.

vonCanstein, H., J. Ogawa, S. Shimizu, and J. R. Lloyd. 2008. Secretion of flavins by *Shewanella* species and their role in extracellular electron transfer. Applied and Environmental Microbiology. **74:**615-623.

Vu, B., M. Chen, R. J. Crawford, and E. P. Ivanova. 2009. Bacterial Extracellular Polysaccharides Involved in Biofilm Formation. Molecules. **14:**2535-2554.

Wang, C. J., L. Harper, and W. Z. Cande. 2006. High-resolution single-copy gene fluorescence *in situ* hybridization and its use in the construction of a cytogenetic map of maize chromosome 9. The Plant Cell. **18:**529-544.

Watanabe, K. 2008. Recent Developments in Microbial Fuel Cell Technologies for Sustainable Bioenergy. Journal of Bioscience and Bioengineering. **106:**528-535.

V. J. Watson, and B. E. Logan. 2010. Analysis of polarization methods for elimination of power overshoot in microbial fuel cells. Electrochemistry Communications. **13:**54-56.

Yeung, C. W., M. Woo, K. Lee, and C. W. Greer. 2011. Characterization of the bacterial community structure of Sydney Tar Ponds sediment. Canadian Journal of Microbiology. **57:** 493-503.

Zhang, H., B. E. Logan, J. M. Regan, L. A. Achenbach and M. A. Bruns. 2005. Molecular Assessment of Inoculated and Indigenous Bacteria in Biofilms from a Pilot-Scale Perchlorate-Reducing Bioreactor. Microbial Ecology. **49**:388-398.

Zhang, Y., B. Min, L. Huang, and I Angelidaki. 2009. Generation of Electricity and Analysis of Microbial Communities in Wheat Straw Biomass-Powered Microbial Fuel Cells. Applied Environmental Microbiology. **75:**3389-3395.

Zhao, Y., Y. Chen, D. Zhang, and X. Zhu. 2010. Waste activated sludge fermentation for hydrogen production enhanced by anaerobic process improvement and acetobacteria inhibition. The role of fermentation pH. Environmental Science and Technology. **44:**3317-3323.

Zhen, H., S. D. Minteer, and A. Largust. 2005. Electricity Generation from Artificial Wastewater Using an Upflow Microbial Fuel Cell. Environmental Science and Technology **39:**5262-5267.

Zuo, Y., D. Xing, J. M. Regan, and B. E. Logan. 2008.Isolation of the exoelectrogenic Bacterium *Ochrobactrum anthropi* YZ-1 by using a U-tube microbial fuel cell. Applied and Environmental Microbiology. **74:**3130-3137.